Calculating Transition Rates via Quantum Normal Forms

university of groningen / faculty of science and engineering

Daniel van Dyk

First supervisor: Prof. D. Boer
Second supervisor: Prof. H. Waalkens

2024

Abstract

This thesis investigates the application of normal forms for computing transition rates from a meta-stable potential well over an anharmonic barrier. The method of normal forms allows one to find approximate, local constants of motion around stationary points by performing a perturbative expansion on the level of the Hamiltonian. This facilitates the efficient study of local dynamics and quantities of perturbed systems, such as the energy spectrum and partition function. Classical normal forms (CNF) and its quantum mechanical analogue (QNF) are functionally introduced, along with traditional methods to compute the transition rate of non-interacting systems, such as the path integral (PI). The PI and QNF approaches are compared in calculating the partition function of a quartic-perturbed potential. Finally, the computational results of a QNF Mathematica script are presented for the transition rates of various interacting systems.

Acknowledgements

I must express sincere gratitude to my two supervisors, Profs. Boer and Waalkens, who have together made this thesis possible. Their insights arise from different fields of expertise, and so complemented one another, which allowed me to gain a broader and more nuanced understanding of the subject matter. I further thank Prof. Boer for his efforts in managing my progress and the practicalities of the project.

Additionally, I am indebted to Giovanni van Marion, who made a great effort to introduce me to his Mathematica code, the project as a whole, and to consolidate his notes, which were crucial to many sections of this thesis. Indeed, it his his work that this thesis seeks to conserve and present for future endeavors. The Master's thesis of Robbert W. Scholtens served as an excellent introduction to normal forms, which, truthfully, was difficult to adapt without losing its quality.

Dedication

To my brother, in whose love I persevere. To my father, on whose shoulders I stand. To my mother, in whose spirit I strive.

Contents

1 Introduction

The origin of this work lies in the investigation of normal form transition state theory (NF-TST) in application to problems in the field of physics. 'Normal form' refers to the mathematical method of diagonalizing the Hamiltonian of a system around a stationary/equilibrium point, done order-by-order of the expansion of the system's potential. This comes in two flavours: classical normal form (CNF) and quantum normal form (QNF). Transition state theory (TST) is a well-known approach used to understand the dynamics of chemical reactions characterised by the crossing of an energy barrier. Passing over this barrier with minimal energy means briefly occupying the stationary point - known in TST as the transition state (TS). Employing the normal form (NF) methods here allows one to study the dynamics around the TS, thus providing predictions of canonical quantities, such as the partition function and transition rate constant. TST is a broad field of study in itself, that will not be included in this work.

This thesis is based on the unfinished investigations of Giovanni van Marion, who sought to apply the principles of TST and the methods of normal forms to describe certain processes in quantum field theory (QFT) - namely of phase transitions such as those relating to the sphaleron. The goal of this work is rather more modest; it is to provide a physicists' handbook on the methods of CNF and QNF in the context of calculating transition rates of a meta-stable well (see figure 1.1). In this, it is hoped to consolidate the basis of this aspect of van Marion's work for future investigations to be attempted.

First, an overview of the NF methods is given, with explicit example of calculating the energy spectrum of an anharmonic oscillator. A brief discussion on asymptotic series and truncation error is followed by an attempt to express the perturbed energy spectrum through Feynman diagrams. Secondly, a chapter is given to discussing non-interacting (harmonic) systems - those without anharmonic terms or mode couplings - both classical and quantum mechanical. Here, exact solutions to the partition function and transition rates are derived via a number of methods, including the path integral method. Third and last is a chapter on interacting systems - those with anharmonic terms and/or mode couplings present - for which two perturbative methods are compared: path integral perturbation theory (PI-PT), and QNF perturbation theory (QNF-PT). Particularly, QNF-PT is implemented within Mathematica scripts developed by van Marion, to render transition rates for a variety of interacting (QM) systems. These results are presented in comparison to the classical and quantum transition rates of the non-interacting (harmonic) case. Among the aspects investigated are the QNF-PT truncation error, inclusion of coupled modes, and perturbation strength.

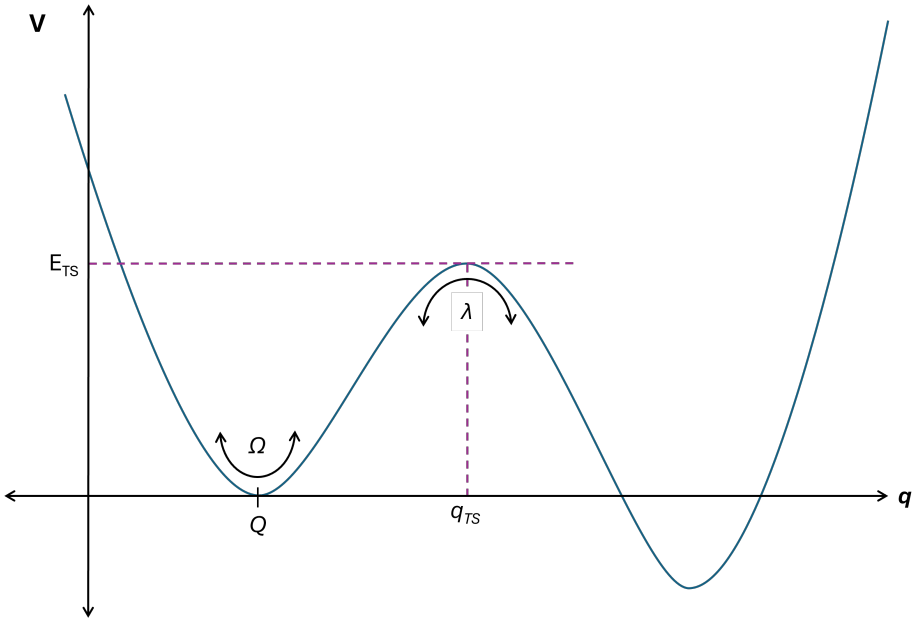

Figure 1.1: A one-dimensional, heuristic depiction of the system of interest. It is composed of a 'false vacuum' - a local minimum containing meta-stable states, a 'true vacuum' - a lower, unpopulated minimum, and an energy barrier separating the two.

2 The Normal Form Method

Much has been written about the classical Birkhoff Gustavson normal form (CNF) and its quantum theory extension (QNF) [16], [8]. Its purpose is to find the local, approximate constants of motion around an equilibrium/stationary point of a system, thus allowing one to gain insight into the dynamics around these points. This work will provide a functional overview of the method and provide illustration through explicit calculation of the QNF of a quartic-perturbed harmonic oscillator. To this end, the thesis of Robbert W. Scholtens [20] provides an accessible and comprehensive introduction to the subject, and is the model upon which the first three sections of this chapter are based.

2.1 CNF

We aim to write the Hamiltonian of our system as a perturbative expansion (in phase-space variables p, q) around the equilibrium point.This is achieved by applying successive symplectic transformations to a Hamiltonian that is expanded up to a term of desired **homogeneous order**, until the desired **normal order** is reached (not to be confused with normal order*ing* in quantum mechanics). Let us begin, then, by defining these terms.

2.1.1 Classical Homogeneous Order

$$\mathcal{W}^n := \mathsf{span}\{q^\alpha p^\beta : \alpha, \beta \in \mathbb{N}_0 \text{ and } \alpha + \beta = n\} \tag{2.1}$$

is the space of polynomials of *homogeneous order n*, defined over $\mathbb{C}$.

2.1.2 Classical Normal Order

For a Hamiltonian H with an equilibrium/stationary point at $z_0 = (p_0, q_0)$, such that $\nabla H(z_0) = 0$, and H_2 be its Taylor expansion to homogeneous order 2, then H is in **classical normal form** *up to order m* around z_0 if

$$\{H_2, H\} = 0 + \mathcal{O}_{ho}(m+1) \tag{2.2}$$

where $\{\cdot,\cdot\}$ denotes the Poisson bracket, and $\mathcal{O}_{ho}$ indicates homogeneous order over p, q.

Very rarely will a Hamiltonian be in CNF up to order > 2. Therefore we search for a (series of) transformation(s) that will increase the normal order of our Hamiltonian; $W_m \in \mathcal{W}^m, m \geq 3$. The functions W_m are the generators of the Hamiltonian flow $\Phi^t_{W_m}$, which defines the symplectic transformations necessary to simplify, or 'normalize' the Hamiltonian, while maintaining its structure. This transformation can be written as the following expansion:

$$H^{(m)} = \sum_{j=0}^{\infty} (j!)^{-1} (\mathsf{ad}_{W_m})^j H^{(m-1)}. \tag{2.3}$$

Here, $\mathrm{ad}_{W_m} H := \{W_m, H\}$ denotes the adjoint action. The expanded Hamiltonian terms of different homogeneous orders are related by the following:

$$H_h^{(m)} = \sum_{j=0}^{\lfloor h/(m-2) \rfloor} (j!)^{-1} (\mathrm{ad}_{W_m})^j H_{h-j(m-2)}^{(m-1)} \tag{2.4}$$

where we note:

1. $H_h^{(m)} = H_h^{(m-1)}$, for all $m \geq 3$ and $0 \leq h < m$,
2. $H_2^{(m)} = H_2^{(2)}$ for all $m \geq 3$.

Importantly, the transformations will never affect those terms already fixed by previous transformations - they can only increase the normal order (see figure 2.1). A proof of this, and derivations to (2.3), (2.4) can be found in [16].

$$\begin{array}{lccccccccccc}
 & H & = & H_{0,1,2} & + & H_3 & + & H_4 & + & H_5 & + & H_6 & + & \cdots \\
W_3 & \downarrow & & & & & & & & & & & & \\
 & H^{(3)} & = & H_{0,1,2}^{(3)} & + & H_3^{(3)} & + & H_4^{(3)} & + & H_5^{(3)} & + & H_6^{(3)} & + & \cdots \\
W_4 & \downarrow & & & & & & & & & & & & \\
 & H^{(4)} & = & H_{0,1,2}^{(4)} & + & H_3^{(4)} & + & H_4^{(4)} & + & H_5^{(4)} & + & H_6^{(4)} & + & \cdots \\
W_5 & \downarrow & & & & & & & & & & & & \\
 & H^{(5)} & = & H_{0,1,2}^{(5)} & + & H_3^{(5)} & + & H_4^{(5)} & + & H_5^{(5)} & + & H_6^{(5)} & + & \cdots \\
W_6 & \downarrow & & & & & & & & & & & & \\
 & H^{(6)} & = & H_{0,1,2}^{(6)} & + & H_3^{(6)} & + & H_4^{(6)} & + & H_5^{(6)} & + & H_6^{(6)} & + & \cdots \\
W_7 & \downarrow & & & & & & & & & & & & \\
 & \vdots & & & & & & & & & & & & \ddots
\end{array}$$

Figure 2.1: An illustration of the iterative nature of the normal form method, taken from [20]. Terms of like colour (except black) are equal.

2.1.3 The Homological Equation

For the case that $H^{(N-1)}$ is in CNF up to order $N-1$, $N \geq 3$, to ensure $H^{(N)}$ is in CNF up to order N, then the following condition is placed on $W_N \in \mathcal{W}^N$:

$$H_N^{(N-1)} - \mathcal{D}W_N \in \ker\mathcal{D} \tag{2.5}$$

which is the **homological equation**, where $\mathcal{D} := \{H_2^{(2)}, \cdot\} : \mathcal{W}^N \to \mathcal{W}^N$ is the **homological operator**. Finding successive W_N's can be tricky, as will be illustrated later. With this basic scaffolding, however, we can now look at the quantum adaptation and then an application.

2.2 QNF

Because working in phase space, where functions commute, is computationally easier than working in Hilbert space, where operators do not commute, the strategy of the

QNF algorithm will be to compute normal forms using phase-space *symbols*, then to quantize to *operators* (make a Weyl transform) at the end. To do so, we follow the work of Hilbrand J. Groenewold and José E. Moyal. Introducing the **star product**:

$$A \star B := \sum_{j=0}^{\infty} \frac{1}{j!} \Big(\frac{i\hbar}{2}\Big)^j A[\overleftarrow{\partial}_q \overrightarrow{\partial}_p - \overleftarrow{\partial}_p \overrightarrow{\partial}_q]^j B = AB + \frac{1}{2} i\hbar\{A, B\} + \mathcal{O}(\hbar^2) \tag{2.6}$$

where A and B are two 'operatorfied' state space functions. This gives us the relations

$$\mathsf{Op}[A]\mathsf{Op}[B] = \mathsf{Op}[A \star B] \tag{2.7}$$

$$[\mathsf{Op}[A], \mathsf{Op}[B]] = \mathsf{Op}[A]\mathsf{Op}[B] - \mathsf{Op}[B]\mathsf{Op}[A] = \mathsf{Op}[A \star B - B \star A] \tag{2.8}$$

which will be used once we have transformed our Hamiltonian to the desired normal order, to then obtain an energy spectrum. We should further heed what Groenewold observed [2], that any quantization of the Poisson bracket of functions on phases space is precise only to first order in $\hbar$. Therefore, we introduce the **Groenewold-Moyal bracket**:

$$\begin{aligned}\{A, B\}_M := -i\hbar^{-1}(A \star B - B \star A) = \sum_{j=0}^{\infty} \frac{(-1)^j (\frac{1}{2}\hbar)^{2j}}{(2j+1)!} A[\overleftarrow{\partial}_q \overrightarrow{\partial}_p - \overleftarrow{\partial}_p \overrightarrow{\partial}_q]^{2j+1} B \\ = \{A, B\} + \mathcal{O}(\hbar^2)\end{aligned} \tag{2.9}$$

with state space functions A and B, and further, $\mathsf{Mad}_A B := \{A, B\}_M$ as the **Groenewold-Moyal adjoint action**. We note two details; that the higher order terms disappear when either A or B are of hom. order 2, and that setting $\hbar \equiv 0$ reduces this to the Poisson bracket.

2.2.1 Quantum Homogeneous Order

$$\mathcal{W}_{QM}^n := \mathsf{span}\{\hbar^\gamma q^\alpha p^\beta : \alpha, \beta, \gamma \in \mathbb{N} \text{ and } \alpha + \beta + 2\gamma = n\} \text{ over } \mathbb{C} \tag{2.10}$$

defines the space of polynomials of quantum homogeneous order (qho) n.

2.2.2 Quantum Normal Order

Respecting the preceding discussion, we consider a phase-space *symbol* H (of which the $\hbar$-independent terms can be considered to be the classical Hamiltonian) with an equilibrium point at the origin, $(q, p) = (0, 0)$, and H_2 to be its Taylor expansion up to qho 2. Then H is in quantum normal form (QNF) up to order N if

$$\{H_2, H\}_M = 0 + \mathcal{O}_{qho}(N + 1). \tag{2.11}$$

Similarly as for the classical case, where we wished to represent the series of transformations that gave us a Hamiltonian of CNF order N as an expansion, now we see that the Poisson adjoint action of (2.3) is replaced with the Moyal adjoint action:

$$H^{(m)} = \sum_{j=0}^{\infty} (j!)^{-1} (\mathsf{Mad}_{W_m})^j H^{(m-1)} \tag{2.12}$$

but is otherwise the same. The Moyal adjoint is what will introduce powers of $\hbar$ to our Hamiltonian expansion, which is otherwise done completely in a classical setting. The equation relating Hamiltonian terms (2.4) also needs revision:

$$H_h^{(m)} = \sum_{j=0}^{\lfloor h/(m-2)\rfloor} (j!)^{-1} (\mathsf{Mad}_{W_m})^j H_{h-j(m-2)}^{(m-1)} \tag{2.13}$$

however, the homological equation remains the same, only that it now refers to transformations that act as described in (2.12).

2.3 Bringing the Anharmonic Oscillator/Barrier to QNF Order 4

The context of this work inspires us to look at the case of two potential wells separated by a barrier. The well and barrier may each be described as harmonic with quartic perturbations. Our strategy is to look at the Taylor expansion of our Hamiltonian order by order and perform transformations that 'normalize' each term. We take $H = p^2 + V(q)$, with $V(q) = aq^2 + bq^4$ and $V'(0) = 0$. The Maclaurin expansion is then

$$H = p^2 + V_0 + \frac{1}{2}V''(0)^2 q^2 + \sum_{j=3}^{\infty} \frac{V^{(j)}(0)}{j!} q^j. \tag{2.14}$$

We can conveniently rewrite this as

$$H = p^2 + V_0 - \frac{1}{4}\lambda^2 q^2 + \sum_{j=3}^{\infty} \frac{V^{(j)}(0)}{j!} q^j \tag{2.15}$$

taking $\lambda := \sqrt{-2V''(0)}$, for the following reason. Note that

$$\begin{aligned} p^2 - \frac{1}{4}\lambda^2 q^2 &= (p + \frac{1}{2}\lambda q)(p - \frac{1}{2}\lambda q) \\ &= \lambda \underbrace{(\lambda^{-1/2} p + \frac{1}{2}\lambda^{1/2} q)}_{=:\tilde{q}} \underbrace{(\lambda^{-1/2} p - \frac{1}{2}\lambda^{1/2} q)}_{=:\tilde{p}} \end{aligned} \tag{2.16}$$

which allows us, by a simple coordinate transformation, to combine the two terms at quantum homogeneous order 2 into one term, $\lambda\tilde{p}\tilde{q}$. Thus

$$H = V_0 + \lambda\tilde{q}\tilde{p} + \sum_{j=3}^{\infty}\sum_{l=0}^{j} C_{j,l}\tilde{q}^l\tilde{p}^{j-l} \tag{2.17}$$

with

$$C_{j,l} := \frac{(-1)^{j-l}V^{(j)}(0)}{(j-l)!l!\lambda^{j/2}} \tag{2.18a}$$

$$C_{j,l} = (-1)^l \binom{j}{l} C_{j,0} \tag{2.18b}$$

where we have made use of the common factor of the jth derivative of $V(0)$ for varying l. Henceforth, we will drop the tilde notation for the coordinates p and q, for neatness sake.

Already we have the Hamiltonian in QNF to order 2, at qho 2: $H = V_0 + (2i\sqrt{a})pq$. To bring H to QNF order 3, we find the homological operator, $\mathcal{D} := \{H_2^{(2)}, \cdot\} = \{\lambda pq, \cdot\}$. Since we have fashioned our Taylor expansion to give us terms of $q^l p^{j-l}$, we also want to express the homological operator in a basis of qho 3 eigenvectors: $\{q^3, q^2p, qp^2, p^3, \hbar q, \hbar p\}$. Therefore,

$$\mathcal{D} = \{\lambda pq, \cdot\} = \lambda p\frac{\partial}{\partial p} - \lambda q\frac{\partial}{\partial q} \equiv \lambda \mathsf{diag}(-3, -1, 1, 3, -1, 1). \tag{2.19}$$

This diagonal matrix has no zero entries, so it is straightforward to find its inverse:

$$\mathcal{D}^{-1} = \frac{1}{\lambda}\mathsf{diag}(-\frac{1}{3}, -1, 1, \frac{1}{3}, -1, 1). \tag{2.20}$$

Then from the homological equation (2.5) we find $W_3 = \mathcal{D}^{-1}H_3^{(2)}$. Using the equation relating Hamiltonian terms (2.13), we see

$$\begin{aligned} H_3^{(3)} &= H_3^{(2)} + \mathsf{Mad}_{W_3}H_2^{(2)} + \frac{1}{2}(\mathsf{Mad}_{W_3})^2H_1^{(2)} + \frac{1}{6}(\mathsf{Mad}_{W_3})^3H_0^{(2)} \\ &= H_3^{(2)} + \mathsf{Mad}_{W_3}H_2^{(2)} \end{aligned} \tag{2.21}$$

since the last two terms are zero. The first term is the Hamiltonian expanded to homogeneous order 3, at quantum normal order 2, and the second term reduces to the Poisson adjoint due to $H_2^{(2)}$ being of homogeneous order 2.

Performing the expansion, one finds the terms at homogeneous order 3 can be written in our previously chosen basis as $H_3^{(2)} \equiv (C_{3,3}, C_{3,2}, C_{3,1}, C_{3,0}, 0, 0)^T$. The coefficients $C_{3;l} = 0$ for $V(q) = aq^2 + bq^4$. Then $W_3 = \mathcal{D}^{-1}H_3^{(2)} = 0$, and right away we have

$$H_3^{(3)} = H_3^{(2)} - \mathcal{D}W_3 = 0 \tag{2.22}$$

which says that at the third qho, the QNF of our Hamiltonian is zero.

Suppose that $C_{3;l} \neq 0$, then a full working of the problem would show W_3 to be

$$W_3 = \mathcal{D}^{-1}H_3^{(2)} = \lambda^{-1}[-\frac{1}{3}C_{3,3}q^3 - C_{3,2}q^2p + C_{3,1}qp^2 + \frac{1}{3}C_{3,0}p^3] \tag{2.23}$$

allowing the calculation of $\mathsf{Mad}_{W_3}H_2^{(2)}$ as follows (with $H_2^{(2)} = \lambda pq$):

$$\begin{aligned} \mathsf{Mad}_{W_3}H_2^{(2)} &= \{W_3, H_2^{(2)}\} \\ &= \lambda^{-1}(-C_{3,3}q^2 - 2C_{3,2}qp + C_{3,1}p^2)(\lambda q) - (\lambda p)(\lambda^{-1}(-C_{3,2}q^2 + 2C_{3,1}qp + C_{3,0}p^2)) \\ &= -C_{3,3}q^3 - C_{3,2}q^2p - C_{3,1}qp^2 - C_{3,0}p^3 \\ &= -\mathcal{D}W_3 \end{aligned} \tag{2.24}$$

such that

$$H_3^{(3)} = H_3^{(2)} - \mathcal{D}W_3 = 0 \tag{2.25}$$

which incidentally agrees with (2.22).

With an eye to reach QNF order 4, let us calculate $H_4^{(3)}$:

$$\begin{aligned} H_4^{(3)} &= H_4^{(2)} + \cancel{\mathsf{Mad}_{W_3} H_3^{(2)}} + \frac{1}{2}(\mathsf{Mad}_{W_3})^2 H_2^{(2)} + \cancel{\frac{1}{6}(\mathsf{Mad}_{W_3})^3 H_1^{(2)}} + \cancel{\frac{1}{24}(\mathsf{Mad}_{W_3})^4 H_2^{(0)}} \\ &= H_4^{(2)} + \frac{1}{2}(\mathsf{Mad}_{W_3}) \underbrace{\mathsf{Mad}_{W_3} H_2^{(2)}}_{-H_3^{(2)}}. \end{aligned} \tag{2.26}$$

A general calculation of the second term via (2.9), provided in A.1, would yield terms $\propto C_{3,0}^2$, but quite thankfully our chosen potential nullifies these, allowing us to go from

$$\begin{aligned} H_4^{(3)} = C_{4,0}[q^4 - 4a^3p + 6q^2p^2 - 4qp^3 + p^4] \\ - C_{3,0}^2\lambda^{-1}[3q^4 + 12q^3p - 30q^2p^2 + 12qp^3 + 12qp^3 + 3p^4 - 4\hbar^2] \end{aligned} \tag{2.27}$$

to the more friendly expression:

$$H_4^{(3)} = H_4^{(2)} = C_{4,0}[q^4 - 4q^3p + 6q^2p^2 - 4qp^3 + p^4] \tag{2.28}$$

with $C_{4,0} = -b/4a$. Expedited by our potential, we are brought to expressing the Hamiltonian at QNF order 4 in its constituents:

$$H_4^{(4)} = H_4^{(3)} + \mathsf{Mad}_{W_4} H_2^{(3)} + \cancel{\frac{1}{2}(\mathsf{Mad}_{W_4})^2 H_0^{(3)}}. \tag{2.29}$$

Indeed, we must find W_4, but that requires finding $\mathcal{D}$ on $\mathcal{W}_{QM}^4$, in an appropriately chosen basis: $\{q^4, q^3p, q^2p^2, qp^3, p^4, \hbar q^2, \hbar qp, \hbar p^2, \hbar^2\}$,

$$\mathcal{D} \equiv \lambda\ \mathsf{diag}(-4, -2, 0, 2, 4, -2, 0, 2, 0). \tag{2.30}$$

Alas, this diagonal matrix has zero entries, and thus is not invertible. However, the homological equation only stipulates that $H_4^{(3)} - \mathcal{D}W_4$ is in the kernel of $\mathcal{D}$. The *Fredholm alternative* [10] allows us to make the splitting: $\mathcal{W}_{QM}^4 = \mathsf{Im}\mathcal{D} \oplus \mathsf{ker}\mathcal{D}$, which in turn implies the Hamiltonian may be split as $H_4^{(3)} = H_{4;\mathsf{Im}}^{(3)} + H_{4;\mathsf{ker}}^{(3)}$. Then, to satisfy the homological equation, we must have that

$$H_4^{(3)} - \mathcal{D}W_4 = H_{4;\mathsf{Im}}^{(3)} + H_{4;\mathsf{ker}}^{(3)} - \mathcal{D}W_4 \overset{!}{\in} \mathsf{ker}\mathcal{D} \quad \Rightarrow \quad H_{4;\mathsf{Im}}^{(3)} - \mathcal{D}W_4 = 0. \tag{2.31}$$

Therefore, we focus our efforts on finding W_4 that satisfies this rightmost equation.

Observe, from the basis elements related to the zero entries of $\mathcal{D}$ ($q^2p^2, \hbar qp$, and $\hbar^2$), that we may identify $H_{4;\mathsf{ker}}^{(3)}$ from (2.27) as:

$$H_{4;\mathsf{ker}}^{(3)} = 6C_{4,0}q^2p^2 \tag{2.32}$$

where we look at (2.28), thus disregarding those terms that would be included by the full expression in (2.27). Similarly for the image:

$$H_{4;\mathsf{Im}}^{(3)} = C_{4,0}\Big[q^4 - 4q^3p - 4qp^3 + p^4\Big]. \tag{2.33}$$

Now we simply consider the reciprocal of those elements in the image of $\mathcal{D}$, i.e. $(-\frac{1}{4}, -\frac{1}{2}, \frac{1}{2}, \frac{1}{4})$, not forgetting the factor of $1/\lambda$, and multiply this to the above equation to solve for W_4:

$$W_4 = \frac{C_{4,0}}{\lambda}\Big[-\frac{1}{4}q^4 + 2q^3p - 2qp^3 + \frac{1}{4}p^4\Big]. \tag{2.34}$$

Finally, calculating $\mathsf{Mad}_{W_4} H_2^{(3)}$, we find it cancels with $H_{4;\mathsf{Im}}^{(3)}$, leaving us with

$$H^{(4)} = V_0 + \lambda pq + H_{4;\mathsf{ker}}^{(3)} + \mathcal{O}_{qho}(5) \tag{2.35}$$

or, for the special case of the quartic perturbation,

$$H^{(4)} = V_0 + 2i\sqrt{a}(pq) - \frac{3b}{2a}(pq)^2 + \mathcal{O}_{qho}(5) \tag{2.36}$$

2.3.1 Even powers of p, q

Though not obvious, the occurrence of even powers of the phase space variables p, q holds generally for 1D potential barriers, such that

$$H^{(N)} = \sum_{j=0}^{\lfloor N/2 \rfloor} \alpha_j I^j + \mathcal{O}_{qho}(N+1) \tag{2.37}$$

for $I := pq$ and constants $\alpha_j = \alpha_j(\hbar)$. A proof of this can be found in [20].

The quantity $I = pq$ is a constant of motion, since it commutes with the Groenewold-Moyal bracket and has no explicit time dependence. Thus, once quantized, I and H will have simultaneous eigenstates, which allows us to know the eigenvalues of H (the energy spectrum E_n in the case of a well, and resonant energies in the case of a barrier) by knowing the eigenvalues of I. By expressing the Hamiltonian as a power series in terms of the constants of motion (around a particular stationary point), we have found a direct path to calculating E_n.

2.4 Energy Spectrum from QNF

Let us, by symplectic/canonical transformations, rewrite our Hamiltonian in (2.14) to be as follows, choosing to focus on a potential *well* rather than a barrier:

$$H = \frac{p^2}{2m} + \frac{1}{2}m\omega^2 q^2 + g_4 q^4 \tag{2.38}$$

with $a \to \frac{m\omega^2}{2}$, $b \to g_4$, and $p \to p/\sqrt{2m}$. Our Hamiltonian is, to fourth order quantum normal form (also employing $I := pq$):

$$H^{(4)} = V_0 + i\omega I - \frac{3g_4}{2m^2\omega^2} I^2. \tag{2.39}$$

To find the energy spectrum, we look to the operator version of the above equation, with associated operators $\mathcal{H}$ and $\mathcal{I}$:

$$\mathcal{H}^{(4)} = \mathsf{Op}[H] = V_0 + iw\mathsf{Op}[I] - \frac{3g_4}{2m^2\omega^2}\mathsf{Op}[I^2] \tag{2.40}$$

where $\mathsf{Op}[I] = \mathcal{I}$, but $\mathsf{Op}[I^2] \neq \mathcal{I}^2$. Recall our definitions at the beginning of this chapter; (2.6), (2.7) and (2.8). which shows that $\mathsf{Op}[I]^2 = \mathsf{Op}[I \star I]$. Developing this out will allow us to relate $\mathsf{Op}[I]^2$ to $\mathsf{Op}[I^2]$:

$$I \star I = I^2 + \frac{i\hbar}{2}\cancel{\{I, I\}} + \frac{1}{2}\left(\frac{i\hbar}{2}\right)^2 I\left[\overleftarrow{\partial_q^2}\overrightarrow{\partial_p^2} + \overleftarrow{\partial_p^2}\overrightarrow{\partial_q^2} - 2\overleftarrow{\partial_q}\overleftarrow{\partial_p}\overrightarrow{\partial_q}\overrightarrow{\partial_p}\right] I$$

$$I \star I = I^2 + \frac{\hbar^2}{4} \tag{2.41}$$

$$\Rightarrow \mathsf{Op}[I^2] = \mathsf{Op}[I \star I - \frac{\hbar^2}{4}] = \mathsf{Op}[I]^2 - \frac{\hbar^2}{4} = \mathcal{I}^2 - \frac{\hbar^2}{4}. \tag{2.42}$$

Therefore we may rewrite equation (2.40) as

$$\mathcal{H}^{(4)} = V_0 + iw\mathcal{I} - \frac{3g_4}{2m^2w^2}(\mathcal{I}^2 - \frac{\hbar^2}{4}). \tag{2.43}$$

Noting that $\mathcal{H}\,|\phi\rangle = E\,|\phi\rangle$ and $\mathcal{I}\,|\phi\rangle = I\,|\phi\rangle$ for the eigenstate ϕ, we immediately have

$$E = V_0 + iwI - \frac{3g_4}{2m^2\omega^2}(I^2 - \frac{\hbar^2}{4}). \tag{2.44}$$

Finally, to reach an expression for the energy spectrum E_n, we can make the substitution $J = iI = \hbar(n + 1/2)$ such that

$$E_n = V_0 + \hbar\omega(n + \frac{1}{2}) + \frac{3g_4}{2m^2\omega^2}\Big(\hbar^2(n + \frac{1}{2})^2 + \frac{\hbar^2}{4}\Big). \tag{2.45}$$

Indeed, the energy spectrum is reduced to that of the harmonic oscillator if the perturbation parameter $g_4 \to 0$. Additionally, we see the result of [3] recreated here for the ground state energy of the quartic-perturbed harmonic oscillator:

$$E_0 = V_0 + \frac{\hbar\omega}{2} + \frac{3}{4}\frac{\hbar^2 g_4}{m^2\omega^2}. \tag{2.46}$$

2.5 Analyticity of the Normal Form Method

The question of the convergence or divergence of the NF method is a difficult one. Cases of convergence are known: [4], [11], however these are in the minority. Usually, one is faced with the question of when to truncate the NF procedure to obtain the desired accuracy - which can be extremely high (see [14], [13], [15]). The QNF procedure illustrated in the previous section generates an asymptotic series with corrections of alternating sign. The true value is thus approached alternately from above and below, though the relative difference between the over/under-estimates and the true value is not known; it may lie closer to the upper or lower approach, and not where we might assume it to be - in the middle of the uncertainty. This uncertainty is dependent on our choice of truncation point. Equation (2.46) shows us the first correction to the quartic-perturbed harmonic oscillator ground state energy. Now consider the energy spectrum of the quartic-perturbed harmonic oscillator, calculated to 18$^{\text{th}}$ normal order via the Mathematica notebooks of van Marion:

$$\begin{aligned} E_0 = \frac{1}{2}\hbar\omega + \frac{3\hbar^2 g_4}{4m^2\omega^2} - \frac{21\hbar^3 g_4^2}{8m^4\omega^5} + \frac{333\hbar^4 g_4^3}{16m^6\omega^8} - \frac{30885\hbar^5 g_4^4}{128m^8\omega^{11}} + \frac{916731\hbar^6 g_4^5}{256m^{10}\omega^{14}} \\ - \frac{65518401\hbar^7 g_4^6}{1024m^{12}\omega^{17}} + \frac{2723294673\hbar^8 g_4^7}{2048m^{14}\omega^{20}} - \frac{1030495099053\hbar^9 g_4^8}{32768m^{16}\omega^{23}} \end{aligned} \tag{2.47}$$

which includes 8 correction terms. Here, there is an accelerating growth of the coefficients, alongside increasing powers of the factor $(\hbar g_4/m^2\omega^3)$, represented by the parameter ϵ in figure 2.2 below. The values of these parameters will tune how quickly

the coefficient growth outstrips the shrinking of the exponentiated parameters (if indeed it is < 1). It is at the turning point - where the successive terms stop shrinking and start growing - that we should consider truncating the series.

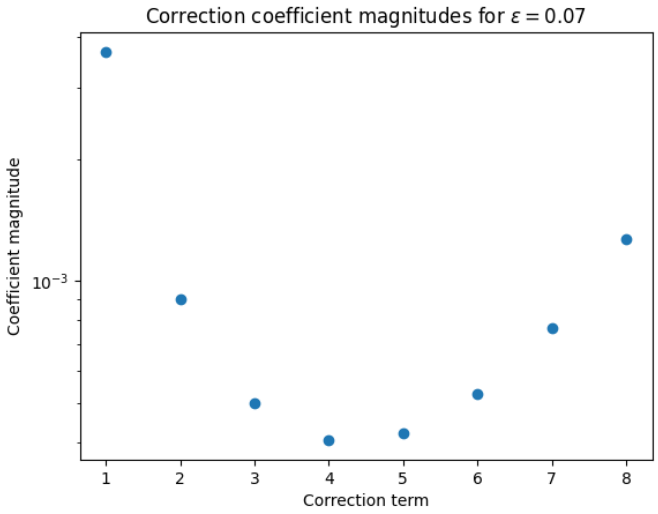

Figure 2.2: The corrections to equation (2.47) begin to grow after the fourth term, for an arbitrarily given parameter ϵ. Truncating the series to end with the third term ensures maximum accuracy.

The optimal truncation rule states that the most accurate result is obtained by summing the asymptotic series up to but not including the smallest term. This ensures that the inherent error imposed by truncating the series is smaller than the last term we added as correction to our approximation. More discussion and illustration on this topic will be presented in a later chapter, where it is applied to the calculation of partition functions and transition rates.

2.6 Diagrammatic Representation of Energy Spectra

The equivalence between Reighley-Schrödinger perturbation theory (RS-PT) and QNF-PT is demonstrated in [19]. The difference is in the treatment of the parameter ϵ, as introduced in figure 2.2: RS-PT treats this as a perturbation parameter, whereas in QNF-PT it is merely a bookkeeping parameter. Only for the ground state can RS-PT be translated to the Feynman diagrams of path integral perturbation theory (PI-PT). This section will demonstrate how one can relate the correlators of excited states of the anharmonic potential to the ground state, thus allowing one to express the excited states in terms of Feynman diagrams.

Consider the Hamiltonian $H = \frac{p^2}{2m} + \frac{1}{2}mw^2q^2 + \frac{g_4}{4!}q^4$. To 6^{th} order in QNF, we have

$$H^{(6)}_{\text{QNF}} = \omega J + \left(\frac{1}{m^2\omega^2}\frac{g_4}{4!}\right)\frac{3}{2}J^2 + \omega\left(\frac{1}{m^2\omega^3}\frac{g_4}{4!}\right)^2\left(\frac{9}{8}\hbar^2 J - \frac{17}{4}J^3\right) \tag{2.48}$$

with $J = iI = ipq$. Performing the Weyl transformation outlined in 2.2 gives us the energy spectrum:

$$E_n^{\text{QNF}} = \hbar\omega(n+1/2) + \hbar^2\Big(\frac{g_4}{4!m^2w^2}\Big)\Big(\frac{3}{2}\Big((n+1/2)^2+\frac{1}{4}\Big)\Big) + \hbar^3\Big(\frac{g_4}{4!m^2\omega^2}\Big)^2\Big(\frac{9}{8}(n+1/2) - \frac{17}{4}\Big((n+1/2)^3+\frac{5}{4}(n+1/2)\Big)\Big). \quad (2.49)$$

In the ordinary perturbation theory (PT) formulation, the same is given by

$$E_n(g_4) = E_n^{(0)} + \frac{g_4}{4!}\langle n^{(0)}|\, x^4\, |n^{(0)}\rangle + \Big(\frac{g_4}{4!}\Big)^2 \sum_{m\neq n} \frac{|\,\langle m^{(0)}|\, x^4\, |n^{(0)}\rangle\,|^2}{E_n^{(0)} - E_m^{(0)}} + \mathcal{O}(g_4^3). \quad (2.50)$$

To evaluate this, we make use of the Feynman rules for the quantum mechanical quartic oscillator, namely:

(2.51)

such that the amplitude of a diagram is composed of a symmetry factor S, and $I = e^{-|\tau-\tau'|}/2$. Take, as an example, a single loop:

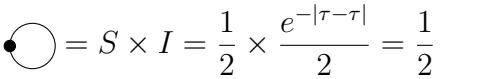

(2.52)

whereas for the double loop:

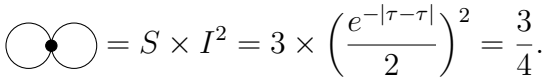

(2.53)

Thus, we write the following relations:

$$\langle 0|\, x^2\, |0\rangle = \sqrt{\frac{m\omega}{\pi\hbar}}\int_{-\infty}^{\infty} x^2 e^{-m\omega x^2/\hbar}dx = \frac{1}{2}\Big(\frac{\hbar}{m\omega}\Big) =$$

(2.54a)

$$\langle 0|\, x^4\, |0\rangle = \sqrt{\frac{m\omega}{\pi\hbar}}\int_{-\infty}^{\infty} x^4 e^{-m\omega x^2/\hbar}dx = \frac{3}{4}\Big(\frac{\hbar}{m\omega}\Big)^2 =$$

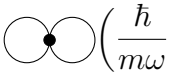

(2.54b)

omitting for the moment the factor $(-g_4/4!)$ associated to each 4-point vertex. We can write the nth excited state as $|n\rangle = \frac{(a^\dagger)^n}{\sqrt{n!}}|0\rangle$, and using the regular definition of the creation/annihilation operators: $a = \sqrt{\frac{m\omega}{2\hbar}}(x + \frac{i}{m\omega}p)$, $a^\dagger = \sqrt{\frac{m\omega}{2\hbar}}(x - \frac{i}{m\omega}p)$, such that $[a, x] = [x, a^\dagger] = \sqrt{\hbar/2m\omega}$. Then, our RS-PT expression for the energy spectrum, at linear order in g_4, becomes

$$E_n(g_4) = E_n^{(0)} + \frac{g_4}{4!n!}\langle 0|\, a^n x^4 (a^\dagger)^n\, |0\rangle\,. \quad (2.55)$$

Let us evaluate the linear correction to the first excited state, and check whether the result agrees with our QNF prediction:

$$\begin{aligned}
\Delta E_1|_{\mathcal{O}(g_4)} &= \frac{g_4}{4!}\langle 0|\, ax^4a^\dagger\,|0\rangle \\
&= \frac{g_4}{4!}\langle 0|\, xax^3a^\dagger\,|0\rangle + \frac{g_4}{4!}\sqrt{\hbar/2m\omega}\,\langle 0|\, x^3a^\dagger\,|0\rangle \\
&= \frac{g_4}{4!}\langle 0|\, x^2ax^2a^\dagger\,|0\rangle + 2\frac{g_4}{4!}\sqrt{\hbar/2m\omega}\,\langle 0|\, x^3a^\dagger\,|0\rangle \\
&= \frac{g_4}{4!}\langle 0|\, x^3axa^\dagger\,|0\rangle + 3\frac{g_4}{4!}\sqrt{\hbar/2m\omega}\,\langle 0|\, x^3a^\dagger\,|0\rangle \\
&= \frac{g_4}{4!}\langle 0|\, x^4aa^\dagger\,|0\rangle + 4\frac{g_4}{4!}\sqrt{\hbar/2m\omega}\,\langle 0|\, x^3a^\dagger\,|0\rangle \\
&= \frac{g_4}{4!}\cancel{\langle 0|\, x^4a^\dagger a\,|0\rangle} + \frac{g_4}{4!}\langle 0|\, x^4\,|0\rangle + 4\frac{g_4}{4!}\sqrt{\hbar/2m\omega}\,\langle 0|\, x^3a^\dagger\,|0\rangle\,.
\end{aligned} \tag{2.56}$$

Evaluating the last term:

$$\begin{aligned}
4\frac{g_4}{4!}\sqrt{\hbar/2m\omega}\,\langle 0|\, x^3a^\dagger\,|0\rangle &= 4\frac{g_4}{4!}\sqrt{\hbar/2m\omega}\left[\,\langle 0|\, x^2a^\dagger x\,|0\rangle + \sqrt{\hbar/2m\omega}\,\langle 0|\, x^2\,|0\rangle\,\right] \\
&= 4\frac{g_4}{4!}\sqrt{\hbar/2m\omega}\left[\,\langle 0|\, xa^\dagger x^2\,|0\rangle + 2\sqrt{\hbar/2m\omega}\,\langle 0|\, x^2\,|0\rangle\,\right] \\
&= 4\frac{g_4}{4!}\sqrt{\hbar/2m\omega}\left[\,\cancel{\langle 0|\, a^\dagger x^3\,|0\rangle} + 3\sqrt{\hbar/2m\omega}\,\langle 0|\, x^2\,|0\rangle\,\right]
\end{aligned} \tag{2.57}$$

$$\Rightarrow \Delta E_1|_{\mathcal{O}(g_4)} = \frac{g_4}{4!}\left(\frac{\hbar}{m\omega}\right)^2 \bigcirc\!\!-\!\!\bigcirc + 6\frac{g_4}{4!}\left(\frac{\hbar}{m\omega}\right)^2 \bullet\!\!\bigcirc = \frac{g_4}{4!}\left(\frac{\hbar}{m\omega}\right)^2 \cdot \frac{15}{4} \tag{2.58}$$

where we identify the two-point and four-point correlators, and thus the appearance of the two aforementioned loop diagrams. Thus we see how the results of QNF-PT correspond to those of the separate PI-PT terms.

What about the corrections at quadratic order? Firstly, we need a general expression for $\langle m|\, x^k\,|n\rangle$ (the derivation is relegated to the Appendix A.2):

$$\langle m|\, x^k\,|n\rangle = \frac{1}{\sqrt{m!n!}}\sum_{j=0}^{\min\{m,n\}} j!\binom{m}{j}\binom{n}{j}\langle 0|\left(\sqrt{\frac{\hbar}{2m\omega}}\frac{d}{dx}\right)^{m+n-2j} x^k\,|0\rangle\,. \tag{2.59}$$

Now we are ready to compute the energy corrections to second order in g_4:

$$E_0 = \frac{\hbar\omega}{2} + \frac{g_4}{4!}\langle 0|\, x^4\,|0\rangle + \left(\frac{g_4}{4!}\right)^2\sum_{k\neq 0}\frac{|\,\langle k|\, x^4\,|0\rangle\,|^2}{\hbar\omega(0-k)} \tag{2.60}$$

$$= \frac{\hbar\omega}{2} + \frac{g_4}{4!}\langle 0|\, x^4\,|0\rangle + \left(\frac{g_4}{4!}\right)^2\left[\frac{|\,\langle 2|\, x^4\,|0\rangle\,|^2}{\hbar\omega(0-2)} + \frac{|\,\langle 4|\, x^4\,|0\rangle\,|^2}{\hbar\omega(0-4)}\right] \tag{2.61}$$

where k selects only values 2 and 4, since by equation (2.59) $k = 1, 3$ give null

contributions. Continuing,

$$E_0 = \frac{\hbar\omega}{2} + \frac{g_4}{4!}\Big(\frac{\hbar}{m\omega}\Big)^2\Big(\frac{3}{4}\Big) + \Big(\frac{g_4}{4!}\Big)^2\Bigg[\frac{1}{-2\hbar\omega}\Big(\frac{12}{\sqrt{2!}}\frac{\hbar}{2m\omega}\left\langle 0\right| x^2 \left|0\right\rangle\Big)^2 + \frac{1}{-4\hbar\omega}\Big(\frac{24}{\sqrt{4!}}\Big(\frac{\hbar}{2m\omega}\Big)^2\Big)^2\Bigg] \tag{2.62}$$

$$\Rightarrow E_0 = \frac{\hbar\omega}{2} + \Big(\frac{\hbar}{m\omega}\Big)^2\frac{g_4}{4!}\Big(\frac{3}{4}\Big) + \frac{\hbar^3}{m^4\omega^5}\Big(\frac{g_4}{4!}\Big)^2\Big[-9\Big(\frac{1}{2}\Big)^2 - \frac{3}{8}\Big] \tag{2.63}$$

where we identify the diagrams associated to $3/4$ and $1/2$, and two new four-point diagrams:

$$\frac{3}{8} \equiv \Big(\frac{g_4}{4!}\Big)^2 \tag{2.64}$$

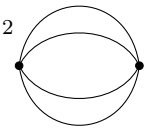

$$\frac{9}{4} \equiv \Big(\frac{g_4}{4!}\Big)^2 \tag{2.65}$$

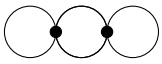

derived by the same methodology from (2.51) and (2.52). This corresponds to the QNF result of (2.49) for $n = 0$:

$$E_0^{\mathsf{QNF}} = \frac{\hbar\omega}{2} + \Big(\frac{\hbar}{m\omega}\Big)^2\frac{g_4}{4!}\Big(\frac{3}{4}\Big) + \frac{\hbar^3}{m^4\omega^5}\Big(\frac{g_4}{4!}\Big)^2\Big(-\frac{21}{8}\Big) \tag{2.66}$$

The traditional employment of Feynman diagrams for problems in quantum field theory (QFT) is limited to calculations in constant backgrounds, such as vacuum-to-vacuum or thermal bath.Calculations of the effects of perturbations to the excited levels of the energy spectrum can only be done by relating said states to the ground state, which, as demonstrated, is neither terribly convenient nor useful. However, general PI-PT (before its translation to Feynman diagrams) is the standard method of calculating partition functions Z and transition rates Γ. This will be illustrated in the coming chapters.

QNF-PT will be presented as a possibly favourable alternative method to be used in the calculation of these quantities, at least in a QM context. Indeed, they yield the same results, but suffer different drawbacks; the major issue with applying QNF-PT to problems in QFT lies in the problem of handling degeneracies in the (infinite-dimensional) Hamiltonian. The presence of a frequency degeneracy increases the size of the kernel of the homological operator $\mathcal{D}$, which results in more terms in the normalized Hamiltonian. These terms make computation of the energy spectrum rather difficult, as they are expressed in angles, not actions, and so the usual substitution of $\hbar$ half-integers is not applicable. The remedy for this is the task of future works - for now we concern ourselves with the successful application of QNF-PT to QM problems.

3 Non-Interacting Systems

We aim to compute the transition (reaction) rate of an interacting quantum system. It is instructive to first review how one might compute the transition rate of a classical, non-interacting system, which will render an analytic solution. Thereafter we can consider how quantum tunneling influences our formulation of the system as a meta-stable canonical ensemble. This will form a firm foundation from which to examine the interacting quantum system. For definiteness we assume the system to consist of a local minimum to the left of a potential barrier, and another, lower minimum on the right. The system is at a nonzero temperature T, such that there is a Boltzmann distribution that allows classical transitions over the barrier, even for the very low lying states of the local minimum (referred to as 'the well' later on).

In this chapter, we restrict ourselves to potential forms that are harmonic near the stationary points of the well and barrier (i.e. no powers higher than q^2), as these can be solved for analytically. Furthermore, there is no interaction, or coupling, between different modes in the form of $q_1 q_2$, and so on. In the next chapter, the QNF algorithm will be employed to deal with anharmonic systems containing interaction terms.

3.1 Classical Rate

Let us set the system to be a meta-stable canonical ensemble. We populate all possible initial coordinates and momenta in the well according to a Boltzmann distribution (at a nonzero temperature). Then, we are looking for the relative fraction of the ensemble that escapes the well per unit time, Γ (i.e. the relative fraction of phase space points that flow out over the barrier).

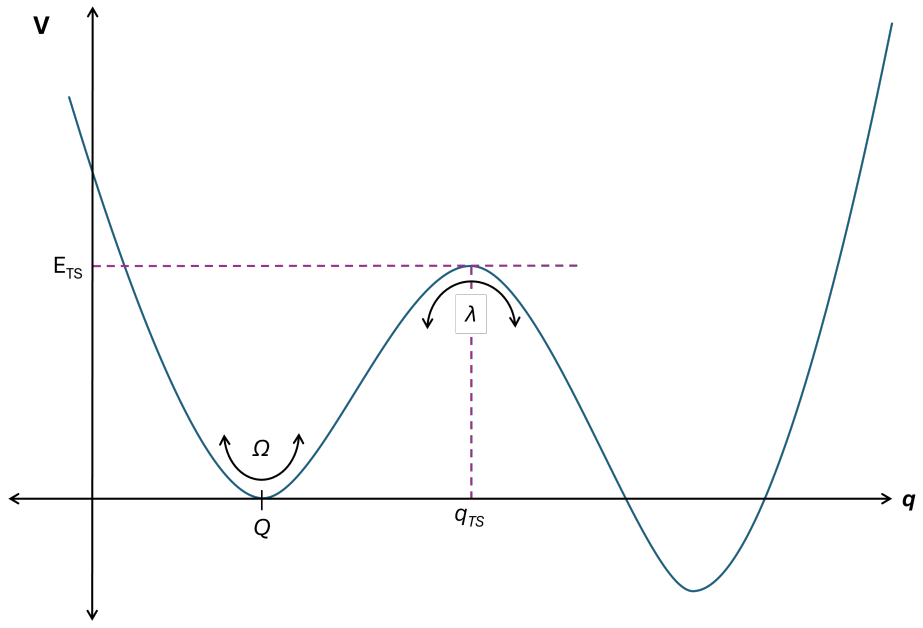

Figure 3.1: A heuristic depiction of the system of interest.

3.1.1 Begin in 1D

Consider first the one-dimensional (1D) system of a metastable well to the left of a barrier, with phase space coordinates (p, q), and $H = p^2/2m + V(q)$ (see figure 3.1). The minimum of the well is set at $q = q_0$, while the barrier (also referred to as the transition state, or TS) is centered at $q = 0$. As many have done before us, such as [5], we can formulate the transition rate as follows:

$$\Gamma = \frac{\int dpdq(2\pi\hbar)^{-1}e^{-\beta H}\delta(q)\cdot(\frac{p}{m})\cdot\Theta(p)}{\int dpdq(2\pi\hbar)^{-1}e^{-\beta H}} = \frac{N(\beta)}{Z(\beta)} \tag{3.1}$$

which describes the probability current across the barrier, where the Heaviside step function $\Theta(p)$ reflects that no particles enter the well from the right (p must be > 0), the Dirac delta $\delta(x)$ selects for the saddle-point, and $Z(\beta)$ is the partition function. The flow along these escaping trajectories is exactly the velocity, $v = p/m$. $\Theta(p)$ will act to reduce the momentum integral to be over only positive momenta (right-going in this setting):

$$\Gamma = \frac{1}{Z}\frac{1}{2\pi\hbar}e^{-\beta E_{TS}}\int_0^\infty dp\cdot pe^{-\beta p^2/2m} = \frac{1}{\beta Z}\frac{1}{2\pi\hbar}e^{-\beta E_{TS}} \tag{3.2}$$

and

$$Z = \int_{-\infty}^{\infty}\frac{dx}{\sqrt{2\pi\hbar}}\int_{-\infty}^{\infty}\frac{dp}{\sqrt{2\pi\hbar}}e^{-\beta(p^2/2+V(q))} = \frac{1}{2\pi\hbar}\sqrt{\frac{2\pi}{\beta}}\int_{-\infty}^{\infty}dqe^{-\beta V(q)}. \tag{3.3}$$

We can approximate $V(q) \approx \frac{\Omega^2}{2}(q-q_0)^2$, being that of the almost-harmonic minimum of the well, and its eigenfrequency Ω, to find

$$\Gamma(\beta)_{\text{classical}} \approx \frac{\Omega}{2\pi}e^{-\beta E_{TS}}. \tag{3.4}$$

Here we see $\Gamma \propto e^{-\beta E_{TS}}$, which some might recognise as the Arrhenius behaviour characteristic of TST reactions [9].

3.1.2 Again in 3D

Fortified by the simplicity of the previous derivation, we now allow our system 3 degrees of freedom (a 6-dim phase space), and distinguish the canonical coordinate pairs near the well (P_n, Q_n) from those near the TS (p_n, q_n). Thus, near the minimum, our Hamiltonian is simply

$$H_0 = \underbrace{\sum_{n=0}^{3}\left(\frac{P_n^2}{2m}+\frac{1}{2}m\Omega_n^2Q_n^2\right)}_{\text{harmonic part}} + \text{interactions we ignore} \tag{3.5}$$

and near the saddle point (TS):

$$H_{TS} = E_{TS} + \underbrace{\frac{p_1^2}{2m}-\frac{1}{2}m\lambda^2q_1^2}_{\text{flipped harmonic part}} + \underbrace{\sum_{n=2}^{3}\left(\frac{p_n^2}{2m}+\frac{1}{2}m\omega_n^2q_n^2\right)}_{\text{regular harmonic part}} + \text{interactions we ignore} \tag{3.6}$$

consistently distinguishing the eigenfrequency near the minimum (Ω_n) from that near the TS (ω_n). Additionally, we take q_1 as the TS reaction coordinate, with eigenfrequency

$\omega_1 \equiv \lambda$, and set the energy of the minimum to 0 and the energy of the barrier to E_{TS}.

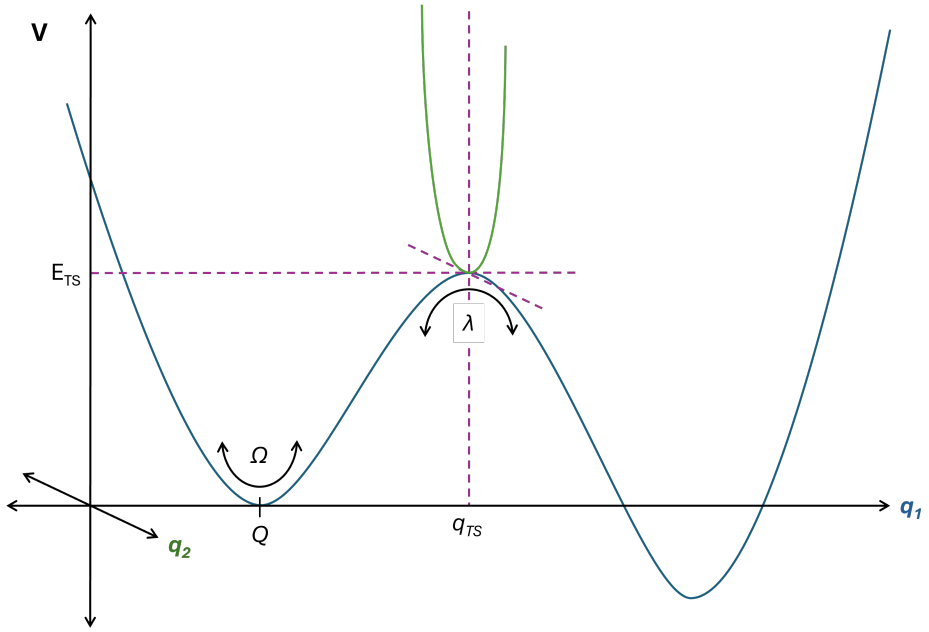

Figure 3.2: Another coordinate axis is added for the q_2 dimension, with corresponding potential depicted in green.

Our 1D formulation (3.1) remains valid, so that we need only consider how the numerator and denominator appear in 3D. Previously, we had normalized to the partition function of the minimum, which is found as the Boltzmann weighted sum over the entire phase space $\mathcal{P} = \mathbb{R}^6$. Now we account for the extra dimensions:

$$Z(\beta) = \int_{\mathcal{P}} \prod_{n=1}^{3} \left(\frac{dP_n dQ_n}{2\pi\hbar} \right) e^{-\beta H_0}. \tag{3.7}$$

This is worked out as

$$Z(\beta) = \int\int_{\mathbb{R}^2} \frac{dP_1 dQ_1}{2\pi\hbar} e^{-\beta\left(\frac{P_1^2}{2m} + \frac{1}{2}m\Omega_1^2 Q_1^2\right)} \times \int\int_{\mathbb{R}^2} \frac{dP_2 dQ_2}{2\pi\hbar} e^{-\beta\left(\frac{P_2^2}{2m} + \frac{1}{2}m\Omega_2^2 Q_2^2\right)} \times \int\int_{\mathbb{R}^2} \frac{dP_3 dQ_3}{2\pi\hbar} e^{-\beta\left(\frac{P_3^2}{2m} + \frac{1}{2}m\Omega_3^2 Q_3^2\right)} = \prod_{n=1}^{3} \left(\frac{1}{\beta\hbar\Omega_n} \right). \tag{3.8}$$

Similarly for the escaping trajectories

$$N(\beta) = \int_{\mathcal{P}} \prod_{n=1}^{3} \left(\frac{dp_n dq_n}{2\pi\hbar} \right) \frac{p_1}{m} \delta(q_1) \Theta(p_1) e^{-\beta H_{TS}} \tag{3.9}$$

$$N(\beta) = e^{-\beta E_{TS}} \int_0^\infty \frac{dp_1}{2\pi\hbar} e^{-\beta\left(\frac{p_1^2}{2m}\right)} \int\int_{\mathcal{R}_2} \frac{dp_2 dq_2}{2\pi\hbar} e^{-\beta\left(\frac{p_2^2}{2m} + \frac{1}{2}m\omega_2^2 q_2^2\right)} \times \int\int_{\mathcal{R}_2} \frac{dp_3 dq_3}{2\pi\hbar} e^{-\beta\left(\frac{p_3^2}{2m} + \frac{1}{2}m\Omega_3^2 q_3^2\right)} = \frac{1}{2\pi\beta\hbar} \prod_{n=2}^{3} \left(\frac{1}{\beta\hbar\omega_n} \right). \tag{3.10}$$

Then the escape rate is:

$$\Gamma(\beta)_{\text{classical}} = \frac{N(\beta)}{Z(\beta)} = \frac{1}{2\pi}\frac{\prod_{n=1}^{3}\Omega_n}{\prod_{n=2}^{3}\omega_n}e^{-\beta E_{TS}} \tag{3.11}$$

which reduces neatly to our result in (3.4) for one dimension. The prefactor says something of the geometry of the system; it measures the relative size of the TS and the minimum. Indeed, a narrower barrier (corresponding to a larger ω_n) decreases the transition rate. Interestingly, the rate does not depend on the barrier eigenfrequency λ, but this also ensures the units of Γ to be per unit time.

3.2 Quantum Rate

For quantum systems we must contend with tunneling contributions to the escape rate. We will revert to the 1D version of the same harmonic Hamiltonians H_0, H_{TS} (now operators), with the TS coordinate $q_{TS} = Q - q$ (dropping subscripts), and retaining the previous definitions for $\Omega_1 \equiv \Omega$ and $\omega_{TS} \equiv \lambda$, such that near the minimum we have

$$H_0 = \underbrace{\left(\frac{P^2}{2m} + \bar{E} + \frac{1}{2}m\Omega^2 Q^2\right)}_{\text{harmonic part}} + \text{interactions we ignore} \tag{3.12}$$

including a shift for the bottom of the well, $\bar{E}$, and near the TS,

$$H_{TS} = E_{TS} + \underbrace{\frac{p^2}{2m} - \frac{1}{2}m\lambda^2 q^2}_{\text{flipped harmonic part}} + \text{interactions we ignore} \tag{3.13}$$

The addition of quantum tunneling to our system with a finitely high barrier means that strictly we cannot have any bound (stationary) wave functions of our states. Therefore, strictly we cannot describe the states of the well as a canonical ensemble (which is a stationary population of levels). However, as we are aiming for the TST regime, wherein the TS is only sporadically occupied, and the barrier is large enough ($\frac{\hbar\Omega}{2}, \frac{\hbar\lambda}{2} \ll E_{TS}$), this meta-stable well can still hold quasi-bound states - the remnants of the harmonic oscillator bound states after perturbative inclusion of the barrier and its tunneling. This approximation leads, in some sense [18], to the states deep inside the well obtaining a small imaginary component to their energies, which describes their tunneling rate [5], γ:

$$\gamma = \frac{2}{\hbar}\text{Im}E. \tag{3.14}$$

Note that the energies of unstable states are not eigenvalues of H, but can only be defined after analytic continuation [7]. If the combined decay rate of the levels is sufficiently small, we can approximate the levels to be in equilibrium, thus producing an almost canonical ensemble in thermal quasi-equilibrium.

A consequence of the preceding discussion is that the partition function, $Z(\beta) = \sum_n e^{-\beta E_n}$, will have an imaginary component. In this low-temperature, high-barrier system, only the lowest lying levels are sufficiently populated. These levels are akin to the harmonic oscillator, and so is the partition function. We thus define the canonical ensemble of a meta-stable well as:

$$Z^{\Omega;\bar{E}}(\beta) = \sum_{n=1}^{\infty} e^{-\beta(\bar{E}+\hbar\Omega(n+1/2))} = \frac{e^{-\beta\bar{E}}}{2\sinh(\frac{\beta\hbar\Omega}{2})}. \tag{3.15}$$

3.2.1 Free Energy and the TST Regime

The quantity we want to find, Γ_{quantum}, is equivalent to the decay rate of the ensemble. These decays can occur via thermal-bath-induced transitions over the barrier or via quantum tunneling. To allow for the quasi-equilibrium description we have adopted, we require $kT = \frac{1}{\beta} \ll E_{TS}$. However, the occupation of the TS that characterizes TST implies that the dominant mode of decay is not via tunneling, but via the TS at $E \approx E_{TS}$. This is reinforced by the locality of the QNF method - that is only accurate within a small neighbourhood of the TS. We therefore wish to find this lower-temperature boundary to fully define the TST regime of validity.

To find Γ_{quantum}, it is necessary to interrupt with a brief look at the Helmholtz free energy, $F(\beta) = -\frac{1}{\beta}\ln(Z(\beta))$, as the following formulations will help us in simplifying the results to come.

The requirement for the well to hold long-lived states, $\text{Re}E \gg \text{Im}E$ carries through to the partition function, $\text{Re}Z \gg \text{Im}Z$. This puts in mind an expansion of the free energy in terms of $\text{Im}Z$:

$$F(\beta) = -\frac{1}{\beta}\ln(\text{Re}Z(\beta)) - \frac{1}{\beta}\frac{\text{Im}Z(\beta)}{\text{Re}Z(\beta)} + \mathcal{O}\Big(\text{Im}Z(\beta)^2\Big)\dots \tag{3.16}$$

Examining the leading order of both the real and imaginary components:

$$\text{Re}F(\beta) = -\frac{1}{\beta}\ln(\text{Re}Z(\beta)) \approx -\frac{1}{\beta}\ln(Z^{\Omega;0}(\beta)) = \frac{\hbar\Omega}{2} + \frac{1}{\beta}\ln(1-e^{\beta\hbar\Omega}) \tag{3.17a}$$

$$\text{Im}F(\beta) = \frac{1}{\beta}\frac{\text{Im}Z(\beta)}{\text{Re}Z(\beta)} \approx \frac{1}{\beta}\frac{\text{Im}Z(\beta)}{Z^{\Omega;0}(\beta)} = -\frac{2}{\beta}\sinh\Big(\frac{\beta\hbar\Omega}{2}\Big)\text{Im}Z(\beta) \tag{3.17b}$$

An analytic continuation of the coordinate integral allows us to evaluate $\text{Im}Z$, using a steepest descent approximation at the TS to write [7]: $V(q) = V_{TS} + \cancel{V'(q_{TS})(q)} + \frac{1}{2}V''(q_{TS})(q^2) + \dots$ such that

$$\text{Im}Z = \frac{1}{\sqrt{\beta\hbar}}\frac{1}{\sqrt{2\pi\hbar}}\int_0^{i\infty} e^{-\beta V(q)}dq \approx \frac{e^{-\beta E_{TS}}}{2}\frac{1}{\beta\hbar\lambda} \tag{3.18}$$

recalling that $\lambda = \omega_{TS} = \sqrt{V''(q_{TS})}$ whereas, as previously alluded to in (3.15),

$$\text{Re}Z \approx \sum_{n=1}^{\infty} e^{-\beta\hbar\Omega(n+1/2)} = \Big[2\sinh(\frac{\beta\hbar\Omega}{2})\Big]^{-1} \approx 1/\beta\hbar\Omega \tag{3.19}$$

valid in the high temperature regime. Thus, at leading order:

$$\text{Im}F(\beta) = \frac{1}{\beta}\frac{\text{Im}Z(\beta)}{\text{Re}Z(\beta)} \approx \frac{\Omega}{2\beta\lambda}e^{-\beta E_{TS}} \tag{3.20}$$

which allows us to rewrite (3.4), now with the quantum corrections, as

$$\Gamma(\beta)_{\text{quantum}} = \frac{\beta\lambda}{\pi}\text{Im}F. \tag{3.21}$$

We identify this as the transition rate of a non-interacting quantum system in the TST regime, $\frac{\hbar\lambda}{2\pi} \ll \frac{1}{\beta} \ll E_{TS}$. The lower bound is explained thusly: taking $\beta = \frac{2\pi}{\hbar\lambda}$, the transition rate becomes [5]

$$\Gamma = \frac{2}{\hbar}\text{Im}F \tag{3.22}$$

which is similar to that of the tunneling rate in (3.14). Note that $\mathrm{Im}F \to \mathrm{Im}E_0$ for very low temperatures. Indeed, we have recovered the expected transition rate at very low temperatures, where tunneling completely dominates. Thus for $\beta \ll \frac{2\pi}{\hbar\lambda}$, the transition rate is given by (3.22), which departs from the TST regime ($\frac{\hbar\lambda}{2\pi} \ll \frac{1}{\beta} \ll E_{TS}$).

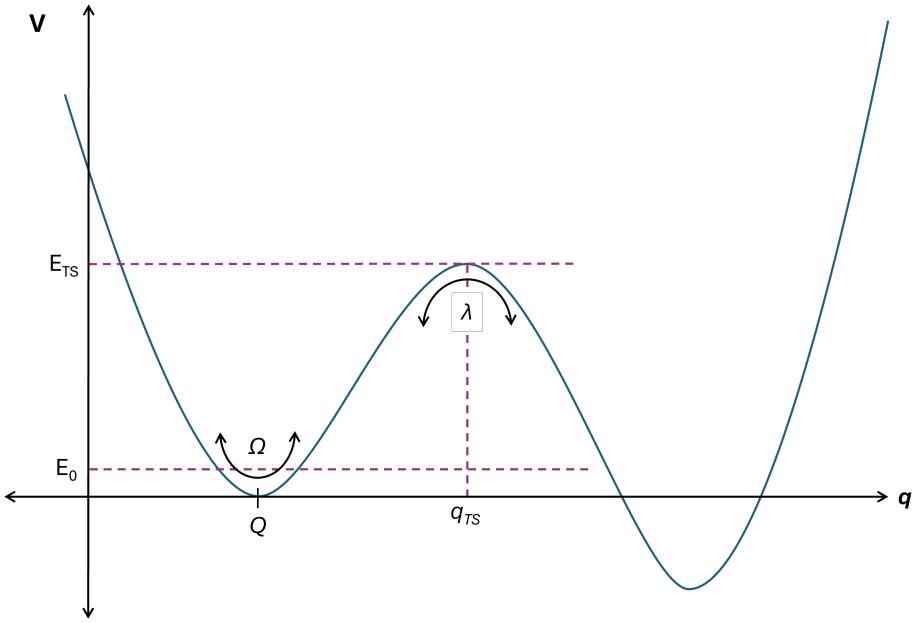

Figure 3.3: Heuristic depiction of the 1-dimensional quantum mechanical system

One might expect there to be a crossover region, where tunneling and scattering contributions become comparable, occurring around $\beta \sim \frac{2\pi}{\hbar\lambda}$. This is indeed the case, and the associated rate becomes more complex, given by a phase transition-like description [5] that we will not discuss here.

3.2.2 WKB Derivation

A general formulation of the transition rate may be given as follows:

$$\Gamma(\beta) = \frac{1}{Z(\beta)} \int_{-\infty}^{\infty} dE \rho(E) \gamma(E) e^{-\beta E} \tag{3.23}$$

with $\rho(E)$ the density of states, and $\gamma(E)$ their tunneling rate. Here, $Z(\beta) = \int_{-\infty}^{\infty} dE \rho(E) e^{-\beta E}$. In the TST regime we are looking at a problem analogous to scattering near the top of the barrier, which is approximately parabolic. This directly corresponds to the known result for the WKB transmission coefficient $T(E)$ of a parabolic barrier [6], [1]:

$$\gamma(E) = T(E) \approx \left[1 + \exp\left(\frac{-2\pi(E - E_{TS})}{\hbar\lambda}\right)\right]^{-1}. \tag{3.24}$$

Next, we consider the density of these scattering states, $\rho(E)$. For $E \approx E_{TS}$, the energy spectrum to the left of the barrier is close to that of the continuum, hence we may write $\rho(E) \approx 1/2\pi\hbar$. Swiftly substituting these values into (3.23), we find:

$$\Gamma(\beta) = \frac{1}{Z(\beta)} \int_{-\infty}^{\infty} dE \frac{1}{2\pi\hbar} \left[1 + \exp\left(\frac{-2\pi(E - E_{TS})}{\hbar\lambda}\right)\right]^{-1} e^{-\beta E}$$

$$= \frac{1}{Z(\beta)} \frac{\lambda}{2\pi} \frac{e^{-\beta E_{TS}}}{2\sin(\frac{\beta\hbar\lambda}{2})}.$$

Furthermore, since $\mathrm{Re}Z \gg \mathrm{Im}Z$ is still valid, so is approximating the partition function to the harmonic oscillator (HO) partition function, $Z(\beta) \approx \mathrm{Re}Z \approx Z_{HO} = [2\sinh(\frac{\beta\hbar\Omega}{2})]^{-1}$. Then:

$$\Gamma(\beta) = \frac{\lambda}{2\pi} \frac{\sinh(\frac{\beta\hbar\Omega}{2})}{\sin(\frac{\beta\hbar\lambda}{2})} e^{-\beta E_{TS}}. \tag{3.25}$$

In the low β, high-temperature regime, this indeed approximates the result obtained earlier (3.21): $\frac{\Omega}{2\pi} e^{-\beta E_{TS}} = \frac{\beta\lambda}{\pi} \mathrm{Im}F$.

3.3 Path Integral Approach

The WKB methods are satisfactory for a proof-of-concept in deriving the partition function and transition rate of a 1D metastable well, but additional dimensions and interactions are better handled by the more powerful, more general *path integral* method. The following sections will detail the basics of this approach as it is applied to the non-interacting/harmonic case, reproducing the results of the previous sections.

Crucially, the methods outlined here will serve as the backbone for calculating transition rates of interacting/anharmonic systems via the perturbative path integral treatment. While the use of Feynman diagrams was shown to not offer much benefit in this regard (see 2.6), general PI-PT still remains the standard tool for deriving solutions to these problems. QNF-PT will serve as the alternate method for calculating perturbation effects on E_n, Z, Γ, and other quantities of interest.

3.3.1 Path Integral Preliminaries

The probability for a particle to travel from an initial position x_i at time t_i to a final position x_f at t_f is given by the transition amplitude kernel $K(x_f, t_f; x_i, t_i)$. There are various ways of expressing this object:

$$\begin{aligned} K(x_f, t_f; x_i, t_i) &= \langle x_f | \, e^{-\frac{i\hat{H}(t_f - t_i)}{\hbar}} \, | x_i \rangle \\ &= \sum_{n=0}^{\infty} \psi_n(x_f)^* \psi_n(x_i) e^{-\frac{iE_n \Delta t}{\hbar}} \\ &= \int_{q(t_i)=x_i}^{q(t_f)=x_f} \mathcal{D}[q] e^{\frac{i}{\hbar} S[q]}. \end{aligned}$$

In the last expression appears the action of the system:

$$S[q] = \int_{t_i}^{t_f} dt L(q(t), \dot{q}(t)) \tag{3.26}$$

involving the Lagrangian $L(q, \dot{q}) = \frac{1}{2} m\dot{q}^2 - V(q)$. Now consider a Wick rotation $\tau = it$, such that we now work with the Euclidean path integral, and Euclidean kernel:

$$K_E(x_f, \tau_f; x_i, \tau_i) = \int_{q(t_i)=x_i}^{q(t_f)=x_f} \mathcal{D}[q] e^{-\frac{1}{\hbar} S[q]}. \tag{3.27}$$

Similarly,

$$S_E[q] = \int_{\tau_i}^{\tau_f} d\tau L_E(q(\tau), \dot{q}(\tau)). \tag{3.28}$$

The Lagrangian is now given by $L_E(q,\dot{q}) = \frac{1}{2}m\dot{q}^2 + V(q)$, where we notice the sign change of the potential. One can now express the partition function of a quantum system as follows:

$$\begin{aligned} Z(\beta) = \sum_{n=0}^{\infty} e^{-\beta E_n} &= \int_{-\infty}^{\infty} dx K_E(x, \beta\hbar; x, 0) \\ &= \int_{q(\beta\hbar)=q(0)} \mathcal{D}[q] e^{-\frac{1}{\hbar}S_E[q]} \end{aligned}$$

where we integrate over all paths beginning and ending in the same system configuration, thus eliminating dependence on the end points, and $\tau_f = \beta\hbar$, $\tau_i = 0$.

This is the path integral expression we must contend with. Exact solutions are few and far between, so it behooves us to use a Gaussian approximation, which for the Euclidean path integral corresponds to an approximation of *steepest descent*. In the case of non-interacting systems, or those with quadratic potentials, this approximation is exact.

3.3.2 Gaussian/Steepest Descent approximation

Consider the path $q(\tau) = \bar{q}(\tau) + \Delta q(\tau)$, consisting of the classical solution to the equations of motion, $\bar{q}(\tau)$, and fluctuations around this path $\Delta q(\tau)$, with fixed end points, so that $\Delta q(\tau_i) = \Delta q(\tau_f) = 0$. These are the *Dirichlet boundary conditions*, which take an alternate form for the partition function: $\Delta q(\beta\hbar) = \Delta q(0)$, and $\int_0^{\beta\hbar} d\tau \Delta q = 0$. The action $S_E[q(\tau)]$ may be treated with the Taylor expansion of a functional to give:

$$\begin{aligned} S_E[\bar{q} + \Delta q] = S[\bar{q}] &+ \int_{\tau_i}^{\tau_f} d\tau_1 \left(\left.\frac{\delta S}{\delta q_1}\right|_{q_1=\bar{q}(\tau_1)} \Delta q(\tau_1) \right) \\ &+ \frac{1}{2}\int_{\tau_i}^{\tau_f} d\tau_1 \int_{\tau_i}^{\tau_f} d\tau_2 \left(\left.\frac{\delta^2 S}{\delta q_1 \delta q_2}\right|_{\substack{q_1=\bar{q}(\tau_1) \\ q_2=\bar{q}(\tau_2)}} \Delta q(\tau_1)\Delta q(\tau_2) \right) + O(\Delta q^3) \end{aligned}$$

using the variation of a functional to write the above as a single $d\tau$ integral, and dropping explicit time dependence notation for Δq:

$$\begin{aligned} = S[\bar{q}] &+ \int_{\tau_i}^{\tau_f} d\tau \left(\left.\frac{\partial L_E}{\partial q}\right|_{q=\bar{q}(\tau)} \Delta q + \left.\frac{\partial L_E}{\partial \dot{q}}\right|_{q=\bar{q}(\tau)} \Delta\dot{q} \right) \\ &+ \frac{1}{2}\int_{\tau_i}^{\tau_f} d\tau \left(\left.\frac{\partial^2 L_E}{\partial^2 q}\right|_{q=\bar{q}(\tau)} \Delta q^2 + 2\left.\frac{\partial^2 L_E}{\partial q \partial \dot{q}}\right|_{q=\bar{q}(\tau)} \Delta q\Delta\dot{q} + \left.\frac{\partial^2 L_E}{\partial \dot{q}^2}\right|_{q=\bar{q}(\tau)} \Delta\dot{q}^2 \right) \\ &+ \mathcal{O}(\Delta q^3). \end{aligned}$$

Rewriting the second term of the first integral using derivative chain rule, one obtains a total derivative term (that vanishes under the integral) and the Euler-Lagrange equation, $\frac{\partial L_E}{\partial q} - \frac{d}{d\tau}\frac{\partial L_E}{\partial \dot{q}}$, which also vanishes for $q = \bar{q}(\tau)$. We are left with the second integral; substituting $L_E = \frac{1}{2}m\dot{q}^2 + V(q)$ gives us

$$= \frac{1}{2}\int_{\tau_i}^{\tau_f} (V''(\bar{q})\Delta q^2 + 0 + m\Delta\dot{q}^2) d\tau$$

where we can note $\Delta\dot{q}^2 = (\partial_\tau \Delta q)(\partial_\tau \Delta q) = (\text{total derivative}) - \Delta q \partial_\tau^2 \Delta q$, such that

$$S_E[q] = S[\bar{q}] + \frac{1}{2}\int_{\tau_i}^{\tau_f} \Big[\Delta q\Big(V''(\bar{q}) - m\partial_\tau^2\Big)\Delta q\Big] d\tau + \mathcal{O}(\Delta q^3). \tag{3.29}$$

Therefore

$$K(x_f, t_f; x_i, t_i) \approx e^{-\frac{1}{\hbar}S_E[\bar{q}]} \times \int \mathcal{D}[\Delta q] e^{-\frac{1}{2}\int_{\tau_i}^{\tau_f} d\tau \Delta q \frac{1}{\hbar}(-m\partial_\tau^2 + V'')\Delta q} \tag{3.30}$$

and

$$Z(\beta) \approx e^{-\frac{1}{\hbar}S_E[\bar{q}]} \times \int \mathcal{D}[\Delta q] e^{-\frac{1}{2}\int_{0}^{\beta\hbar} d\tau \Delta q \frac{1}{\hbar}(-m\partial_\tau^2 + V'')\Delta q} \tag{3.31}$$

imposing the appropriate boundary conditions as described at the beginning of this section.

3.3.3 Path Integrals as Determinants

The term $O \equiv \frac{1}{\hbar}(-m\partial_\tau^2 + V'')$ we recognise to be a Schrödinger operator. Suppose $\phi_n(\tau)$ form an orthonormal basis for O, such that $O\phi_n = \lambda_n \phi_n$, and $\int_0^{\beta\hbar} \phi_n(\tau)\phi_m(\tau)d\tau = \delta_{n,m}$, and that satisfies the boundary conditions $\phi_n(\tau_i) = \phi_n(\tau_f) = 0$ (for $n = 0, 1, ...$). This allows us to expand all variational paths uniquely: $\Delta\phi = \sum_{n=0}^{\infty} a_n \phi_n$. The path integral thus reduces to a regular, infinite-dimensional integral over the amplitudes a_n:

$$\begin{aligned} K_E(x_f, \tau_f; x_i, \tau_i) &\approx e^{-S_E[\bar{q}]} N \prod_{n=0}^{\infty} \int_{-\infty}^{\infty} \frac{da_n}{\sqrt{2\pi}} e^{-\frac{1}{2}\lambda_n a_n^2} \\ &= e^{-S_E[\bar{q}]} N \prod_{n=0}^{\infty} \frac{1}{\sqrt{\lambda_n}} \\ &\equiv e^{-S_E[\bar{q}]} \times N \left[\det_{\substack{\Delta q(\tau_f)=0 \\ \Delta q(\tau_i)=0}} \Big(\frac{1}{\hbar}(-m\partial_\tau^2 + V''(\bar{q})) \Big) \right]^{-1/2} \end{aligned}$$

where we have represented the path integral of the fluctuations around the classical path as a determinant, with the assumption that $\lambda_n > 0$. Here, N accounts for the change $\int \mathcal{D}[\Delta q] \to N \prod_{n=0}^{\infty} \int_{-\infty}^{\infty} da_n$, where we have opted to include a factor of $\frac{1}{\sqrt{2\pi}}$ for each amplitude to neaten the outcome. Similarly,

$$Z(\beta) \approx e^{-S_E[\bar{q}]} \times N \left[\det_{\substack{\Delta q(\beta\hbar)=\Delta q(0) \\ \int_0^{\beta\hbar} \Delta q d\tau = 0}} \Big(\frac{1}{\hbar}(-m\partial_\tau^2 + V''(\bar{q})) \Big) \right]^{-1/2}. \tag{3.32}$$

To find N, consider the kernel of the free particle:

$$K_E(x_f, \tau_f; x_i, \tau_i) = \sqrt{\frac{m}{2\pi\hbar(\tau_f - \tau_i)}} e^{-\frac{1}{\hbar}\frac{m}{2}\frac{(x_f - x_i)^2}{\tau_f - \tau_i}} \tag{3.33}$$

$$= e^{-\frac{1}{\hbar}S_E[\bar{q}]} N \left[\det_{\substack{\Delta q(\tau_f)=0 \\ \Delta q(\tau_i)=0}} \Big(-\frac{m}{\hbar}\partial_\tau^2 \Big) \right]^{-1/2}. \tag{3.34}$$

Taking $x_f = x_i$ results in $S[\bar{q}] = 0$, and a simple rearrangement delivers an expression for N:

$$N = \sqrt{\frac{m}{2\pi\hbar(\tau_f - \tau_i)}} \left[\det_{\substack{\Delta q(\tau_f)=0 \\ \Delta q(\tau_i)=0}} \Big(-\frac{m}{\hbar}\partial_\tau^2 \Big) \right]^{1/2}. \tag{3.35}$$

3.3.4 Path Integral of the Harmonic Oscillator

Consider the one-dimensional harmonic oscillator with $V(Q) = \bar{E} + \frac{1}{2}m\Omega^2 Q^2$, including a shifting term for the minimum, $\bar{E}$. Our strategy will be to find K_E^Ω so that we can calculate $Z(\beta) = \int_{-\infty}^{\infty} dx K_E(x, \beta\hbar; x, 0)$.

Taking $\bar{Q}$ to be the solution to the classical Euclidean equations of motion, we know

$$K_E^\Omega(x_f, \tau_f; x_i, \tau_i) = e^{-\frac{1}{\hbar}S_E[\bar{Q}]} K_E^\Omega(0, \tau_f; 0, \tau_i) \tag{3.36}$$

already implementing the boundary conditions, i.e. zero fluctuation at the end points. Recall that, for harmonic potentials, the Gaussian approximation is exact; the quadratic term in the variation of the action is exactly the action of the fluctuations around the classical path.

Let us put the fluctuations in to determinant form:

$$K_E^\Omega(0, \tau_f; 0, \tau_i) = N \left[\det_{\substack{\Delta q(\tau_f)=0 \\ \Delta q(\tau_i)=0}} \left(\frac{1}{\hbar}(-m\partial_\tau^2 + V''(\bar{q})) \right) \right]^{-1/2}. \tag{3.37}$$

Then using (3.35), we find

$$K_E^\Omega(0, \tau_f; 0, \tau_i) = \sqrt{\frac{m}{2\pi\hbar(\tau_f - \tau_i)}} \left[\frac{\det_{\substack{\Delta q(\tau_f)=0 \\ \Delta q(\tau_i)=0}} \left(-\frac{m}{\hbar}\partial_\tau^2 \right)}{\det_{\substack{\Delta q(\tau_f)=0 \\ \Delta q(\tau_i)=0}} \left(\frac{1}{\hbar}(-m\partial_\tau^2 + V''(\bar{q})) \right)} \right]^{1/2}. \tag{3.38}$$

Next, we wish to compute these determinants. We can assume the form of the orthonormal basis functions ϕ_n for both the numerator and denominator's Schrödinger operators to be Fourier modes. In our case, setting $\tau_i = 0$ without loss of generality:

$$\phi_n(\tau) = \sqrt{\frac{2}{\tau_f}} \sin\left(\frac{n\pi\tau}{\tau_f}\right) \qquad \text{for n=1,2,...} \tag{3.39}$$

therefore

$$\lambda_n^\Omega = \frac{m}{\hbar}\left(\left(\frac{n\pi}{\tau_f}\right)^2 + \Omega^2 \right) \qquad \text{for harmonic particle,} \tag{3.40a}$$

$$\lambda_n^0 = \frac{m}{\hbar}\left(\frac{n\pi}{\tau_f}\right)^2 \qquad \text{for free particle.} \tag{3.40b}$$

Then (3.38) becomes

$$K_E^\Omega(0, \tau_f; 0, 0) = \sqrt{\frac{m}{2\pi\hbar\tau_f}} \left[\frac{\prod_{n=1}^\infty \lambda_n^0}{\prod_{n=1}^\infty \lambda_n^\Omega} \right]^{1/2}. \tag{3.41}$$

Some manipulation gives

$$\begin{aligned} K_E^\Omega(0, \tau_f; 0, 0) &= \sqrt{\frac{m}{2\pi\hbar\tau_f}} \left[\prod_{n=1}^\infty \left(1 - \left(\frac{i\tau_f\Omega}{n\pi} \right)^2 \right) \right]^{-1/2} \\ &= \sqrt{\frac{m\Omega}{2\pi\hbar \sinh(\tau_f\Omega)}} \end{aligned}$$

where the Euler identity $\prod_{n=1}^{\infty}(1-\frac{z^2}{n^2}) = \frac{\sin(\pi z)}{\pi z}$ and the explicit inclusion of a factor of i outlines how the final equality is obtained.

We are almost able to calculate $Z(\beta)$, but we are still missing the classical action, $S_E[\bar{Q}]$. Over the time interval $\tau_i = 0$ to τ_f, it is given by:

$$S_E[\bar{Q}] = \frac{m\Omega}{\hbar}\Big(\coth(\tau_f\Omega)(x_i^2+x_f^2) - \frac{2x_ix_f}{\sinh(\tau_f\Omega)}\Big). \tag{3.42}$$

A derivation of the above is included in A.3. We can reintroduce τ_i to the fluctuations kernel by time shift; since the Hamiltonian is time independent, we can use $\tau_f \to \tau_f - \tau_i$. Then (3.36) becomes

$$K_E^{\Omega}(x_f,\tau_f;x_i,\tau_i) = \sqrt{\frac{m\Omega}{2\pi\hbar\sinh((\tau_f-\tau_i)\Omega)}} \times e^{-\frac{m\Omega}{\hbar}\left(\coth((\tau_f-\tau_i)\Omega)(x_i^2+x_f^2) - \frac{2x_ix_f}{\sinh((\tau_f-\tau_i)\Omega)}\right)} \tag{3.43}$$

and

$$\begin{aligned} Z^{\Omega;0}(\beta) &= \sqrt{\frac{m\Omega}{2\pi\hbar\sinh((\tau_f-\tau_i)\Omega)}}\int_{-\infty}^{\infty} dx K_E^{\Omega}(x,\beta\hbar;x,0) \\ &= \sqrt{\frac{m\Omega}{2\pi\hbar\sinh((\tau_f-\tau_i)\Omega)}}\int_{-\infty}^{\infty} dx e^{-\frac{1}{2}\left(\frac{2m\Omega}{\hbar}\frac{\cosh(\beta\hbar\Omega)-1}{\sinh(\beta\hbar\Omega)}\right)x^2} \\ &= 1/\sqrt{2(\cosh(\beta\hbar\Omega)-1)} = \Big[2\sinh\Big(\frac{\beta\hbar\Omega}{2}\Big)\Big]^{-1}. \end{aligned} \tag{3.44}$$

Indeed this is the result found previously, and expected for the harmonic oscillator system. Retaining a nonzero shift $\bar{E}$ simply recovers (3.15).

One could also calculate $Z(\beta)$ from (3.31), that is, by calculating the classical trajectory of steepest descent, thus finding its contribution to the partition function. This method will run into complications with a zero mode eigenfunction, ϕ_0, as we will see.

Consider $\bar{Q}(\tau) = 0$ to be the solution to the Euclidean equations of motion with potential $-V$. Evidently, this is just the unstable solution pertaining to the *saddle* of the flipped potential V. Consequently, $S_E[\bar{Q}] = 0$. We have already noted that the steepest descent approximation is exact for the harmonic oscillator. Thus,

$$Z^{\Omega;0}(\beta) = N \times \left[\det_{\substack{\Delta q(\beta\hbar)=\Delta q(0)\\ \int_0^{\beta\hbar}\Delta q d\tau = 0}}\Big(\frac{m}{\hbar}(-\partial_\tau^2+\Omega^2)\Big)\right]^{-1/2} \tag{3.45}$$

where N needs to be found anew. For the free particle:

$$\begin{aligned} Z^{0;0}(\beta) = \int_{-\infty}^{\infty} dx K_E^0(x,\beta\hbar;x,0) &= \int_{-\infty}^{\infty}\int_{-\infty}^{\infty}\frac{dpdq}{2\pi\hbar}e^{-\beta\left(\frac{p^2}{2m}\right)} \\ &= \sqrt{\frac{m}{2\pi\beta\hbar^2}}\Big(\int_{-\infty}^{\infty} dx\Big) \\ &= N\left[\det_{\substack{\Delta q(\beta\hbar)=\Delta q(0)\\ \int_0^{\beta\hbar}\Delta q d\tau = 0}}\Big(-\frac{m}{\hbar}\partial_\tau^2\Big)\right]^{-1/2} \end{aligned} \tag{3.46}$$

The eigenfunctions ϕ_n will now include a single constant function:

$$\phi_0(\tau) = 1/\beta\hbar \quad \text{with } \lambda_0^\Omega = \frac{m}{\hbar}\Omega^2,\ \lambda_0^0 = 0 \tag{3.47}$$

and additionally, even and odd plane waves:

$$\tilde{\phi}_n(\tau) = \sqrt{\frac{2}{\beta\hbar}}\cos\left(\frac{2n\pi}{\beta\hbar}\tau\right) \tag{3.48a}$$

$$\bar{\phi}_n(\tau) = \sqrt{\frac{2}{\beta\hbar}}\sin\left(\frac{2n\pi}{\beta\hbar}\tau\right) \tag{3.48b}$$

for $n = 1, 2, \cdots$. These functions share the same eigenvalues:

$$\lambda_n^\Omega = \frac{m}{\hbar}\left(\left(\frac{n\pi}{\beta\hbar}\right)^2 + \Omega^2\right) \qquad \text{for harmonic particle} \tag{3.49a}$$

$$\lambda_n^0 = \frac{m}{\hbar}\left(\frac{n\pi}{\beta\hbar}\right)^2 \qquad \text{for free particle} \tag{3.49b}$$

This allows us to rewrite our expression for the free partition function (3.45) as:

$$Z^{\Omega;0}(\beta) = N\Big[\lambda_0^\Omega \prod_{n=1}^{\infty}(\lambda_n^\Omega)^2\Big]^{-1/2} \tag{3.50}$$

The double degeneracy of the eigenvalues is reflected in the fact that they are squared. Alarm bells rang upon the introduction of $\lambda_0^0 = 0$, which corresponds to the translational invariance of the free system. A similar treatment of (3.46) would have division by 0, and is thus not viable. This divergence also appears in $\int_{-\infty}^{\infty} dx$. The strategy will now be to relate $\int_{-\infty}^{\infty}\frac{da_0}{\sqrt{2\pi}}e^{-\frac{1}{2}\lambda_0^0 a_0^2} = \int_{-\infty}^{\infty}\frac{da_0}{\sqrt{2\pi}}$ to the aforementioned, which will allow for the extraction of the zero eigenvalue from the determinant.

From $\phi_0 x^2 = x^2/\beta\hbar = \lambda_0^0 a_0^2$, note $dx = \sqrt{\beta\hbar}\ da_0$. Then

$$Z^{0;0}(\beta) = \left(\sqrt{\frac{\beta\hbar}{2\pi}}\int_{-\infty}^{\infty} dx\right) N\left[\overline{\det}_{\substack{\Delta q(\beta\hbar)=\Delta q(0)\\ \int_0^{\beta\hbar}\Delta q d\tau = 0}}\Big(-\frac{m}{\hbar}\partial_\tau^2\Big)\right]^{-1/2} \tag{3.51}$$

with $\overline{\det}$ signifying the removal of the zero eigenvalue. Now N can be found as:

$$N = \sqrt{\frac{m}{\beta^2\hbar^3}}\left[\overline{\det}_{\substack{\Delta q(\beta\hbar)=\Delta q(0)\\ \int_0^{\beta\hbar}\Delta q d\tau = 0}}\Big(-\frac{m}{\hbar}\partial_\tau^2\Big)\right]^{1/2} = \sqrt{\frac{m}{\beta^2\hbar^3}}\left[\prod_{n=1}^{\infty}(\lambda_n^0)^2\right]^{1/2} \tag{3.52}$$

Triumphantly, we can return to (3.45) to find:

$$\begin{aligned} Z^{\Omega;0}(\beta) &= \sqrt{\frac{m}{\beta^2\hbar^3}}\left[\frac{\prod_{n=1}^{\infty}(\lambda_n^0)^2}{\lambda_0^\Omega\prod_{n=1}^{\infty}(\lambda_n^\Omega)^2}\right]^{1/2} \\ &= \frac{1}{\beta\hbar\Omega}\left[\frac{\prod_{n=1}^{\infty}(\lambda_n^0)^2}{\lambda_0^\Omega\prod_{n=1}^{\infty}(\lambda_n^\Omega)^2}\right]^{1/2} \\ &= \frac{1}{\beta\hbar\Omega}\left[\prod_{n=1}^{\infty}\left(1-\left(\frac{i\beta\hbar\Omega}{2\pi n}\right)^2\right)\right]^{-1} \\ &= \left[2\sinh\left(\frac{\beta\hbar\Omega}{2}\right)\right]^{-1} \end{aligned} \tag{3.53}$$

in similar fashion to the previous derivation, and with identical result.

The exactness of the Gaussian approximation is lost for more complicated potentials, such as those with cubic or quartic terms. The exactness of the desired quantity is also lost. Hereafter, we must rely on perturbative approaches to obtain non-exact, but hopefully serviceable results for quantities such as Z and Γ. The next chapter follows two such methods: PI-PT and QNF-PT.

4 Interacting Systems

To include anharmonic terms to the system means we must turn to the perturbative methods of either the path integral or QNF frameworks in order to calculate the desired quantities; the partition function Z, and transition rate Γ. This chapter will compare these approaches for finding Z, thereafter honing in on a QNF calculation of Γ. The QNF-PT strategy is put into practice by a Mathematica script, rendering transition rates of 1D and 3D QM systems as a function of temperature. These results are presented, along with a small study on the behaviour of the system under different conditions, namely QNF order, coupling strength, and the inclusion/omission of coupled modes.

4.1 Deriving Z

4.1.1 Z via PI-PT

We begin with a calculation of the partition function Z via a perturbative path integral treatment - that is, by the usual story of Green's functions and functional derivatives (reviews of which can be found in standard texts: [17], [12]):

Take the following Lagrangian to characterise our system:

$$\mathcal{L}_E = \frac{1}{2}m\dot{q}^2 + \frac{1}{2}m\omega^2 q^2 + \underbrace{\frac{g}{4!}q^4}_{\equiv \Delta V} \tag{4.1}$$

with ΔV to be treated as a small perturbation. We define the *periodic n-point correlator*:

$$G_P(\tau_1, \tau_2) = \frac{1}{2m\omega}\frac{\cosh\left[\omega\left(\frac{\beta\hbar}{2} - |\tau_1 - \tau_2|\right)\right]}{\sinh(\frac{\beta\hbar\omega}{2})} \equiv \quad \tau_1 \text{ ———— } \tau_2 \tag{4.2}$$

with external source $J(\tau)$ such that the partition function of a forced harmonic system (without anharmonic term) is given by

$$Z^{\omega;g=0}(\beta|J) = \exp\left(\frac{1}{2\hbar}\int_0^{\beta\hbar} d\tau_1 \int_0^{\beta\hbar} d\tau_2 J(\tau_1) G_P(\tau_1, \tau_2) J(\tau_2)\right) \underbrace{Z^{\omega;g=0}(\beta|J=0)}_{=1/2\sinh(\frac{\beta\hbar\omega}{2})}. \tag{4.3}$$

Then including the perturbation ΔV, and expressing the propagator as functional derivatives with respect to $J(\tau)$ (later taken $= 0$) gives the general expression for our quartic-

perturbed partition function:

$$\begin{aligned} Z^{\omega;g}(\beta|J=0) &= \exp\left[-\frac{1}{\hbar}\int_0^{\beta\hbar} d\tau \Delta V\left(\hbar\frac{\delta}{\delta J(\tau)}\right)\right] Z^{\omega;g=0}(\beta|J)\Big|_{J=0} \\ &= \exp\left[-\frac{1}{\hbar}\int_0^{\beta\hbar} d\tau \frac{g}{4!}\left(\hbar\frac{\delta}{\delta J(\tau)}\right)^4\right] \\ &\quad\times \exp\left(\frac{1}{2\hbar}\int_0^{\beta\hbar} d\tau_1\int_0^{\beta\hbar} d\tau_2 J(\tau_1)G_P(\tau_1,\tau_2)J(\tau_2)\right) \underbrace{Z^{\omega;g=0}(\beta|J=0)}_{=1/2\sinh(\frac{\beta\hbar\omega}{2})}\Big|_{J=0}. \end{aligned} \tag{4.4}$$

We can then expand to first order in g:

$$\begin{aligned} Z^{\omega;g}(\beta|J) &\approx \left[1 - \frac{1}{\hbar}\int_0^{\beta\hbar} d\tau \frac{g}{4!}\left(\hbar\frac{\delta}{\delta J(\tau)}\right)^4 + \mathcal{O}(g^2)\right] \\ &\quad\times \exp\left(\frac{1}{2\hbar}\int_0^{\beta\hbar} d\tau_1\int_0^{\beta\hbar} d\tau_2 J(\tau_1)G_P(\tau_1,\tau_2)J(\tau_2)\right) \underbrace{Z^{\omega;g=0}(\beta|J=0)}_{=1/2\sinh(\frac{\beta\hbar\omega}{2})}\Big|_{J=0} \end{aligned} \tag{4.5}$$

and make the shift $J \to \sqrt{\hbar}J$, such that

$$\begin{aligned} Z^{\omega;g}(\beta|J) &\approx \left[1 - \frac{g\hbar}{4!}\int_0^{\beta\hbar} d\tau \left(\frac{\delta}{\delta J(\tau)}\right)^4 + \mathcal{O}(g^2)\right] \\ &\quad\times \exp\left(\frac{1}{2}\int_0^{\beta\hbar} d\tau_1\int_0^{\beta\hbar} d\tau_2 J(\tau_1)G_P(\tau_1,\tau_2)J(\tau_2)\right) \underbrace{Z^{\omega;g=0}(\beta|J=0)}_{=1/2\sinh(\frac{\beta\hbar\omega}{2})}\Big|_{J=0}. \end{aligned} \tag{4.6}$$

To evaluate this further, we look at the derivative acting on the exponential term:

$$\left(\frac{\delta}{\delta J(\tau)}\right)^4 \exp\left(\frac{1}{2}\int_0^{\beta\hbar} d\tau_1\int_0^{\beta\hbar} d\tau_2 J(\tau_1)G_P(\tau_1,\tau_2)J(\tau_2)\right) = 3G_P(\tau,\tau)^2 = \tag{4.7}$$

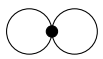

where we take $\tau_1 = \tau_2 = ... = \tau$ coincident, such that

$$G_P(\tau,\tau) = \frac{1}{2m\omega}\frac{\cosh(\frac{\beta\hbar\omega}{2})}{\sinh(\frac{\beta\hbar\omega}{2})} = \frac{1}{2m\omega}\coth\left(\frac{\beta\hbar\omega}{2}\right) = \tag{4.8}$$

Continuing with the evaluation of Z:

$$\begin{aligned} Z^{\omega;g}(\beta|J) &\approx Z^{\omega;g=0}(\beta|J=0)\left[1 - \frac{g\hbar}{4!}\int_0^{\beta\hbar}\Big(3G_P(\tau,\tau)^2 + \mathcal{O}(g^2)\Big)d\tau\right] \\ &= Z^{\omega;\tilde{g}=0}(\beta|J=0)\left[1 - \frac{3}{4}\frac{\tilde{g}\beta\hbar^2}{m^2\omega^2}\coth^2\left(\frac{\beta\hbar\omega}{2}\right) + \mathcal{O}(\tilde{g}^2)\right]. \end{aligned} \tag{4.9}$$

Indeed, we have rendered the quartic-perturbed partition function as an asymptotic series beginning with the exact solution to the unperturbed (harmonic) system, up to the first order correction in the coupling parameter $g/4! = \tilde{g}$.

4.1.2 Z via QNF-PT

Let us now rederive the partition function using the QNF algorithm. Recall that $Z = \sum_{n=0}^{\infty} e^{-\beta E_n}$. We shall take the energy spectrum given by 2.45, restated here:

$$E_n = \hbar\omega(n + \frac{1}{2}) + \frac{3\tilde{g}\hbar^2}{4m^2w^2}(1 + 2n + 2n^2) \tag{4.10}$$

where some simplification has been performed, g_4 was rewritten as $\tilde{g}$ to match the notation of the previous section, and V_0 was set to zero for convenience. We can dive right in:

$$\begin{aligned} Z_{\mathsf{QNF}}^{\omega;\tilde{g}}(\beta) &= \sum_{n=0}^{\infty} \exp\Big(\hbar\omega(n + \frac{1}{2}) + \frac{3\tilde{g}\hbar^2}{4m^2w^2}(1 + 2n + 2n^2)\Big) \\ &= \sum_{n=0}^{\infty} e^{\hbar\omega(n+\frac{1}{2})} \cdot \exp\Big(\frac{3\tilde{g}\hbar^2}{4m^2w^2}(1 + 2n + 2n^2)\Big). \end{aligned} \tag{4.11}$$

Now expanding the second exponential in $\tilde{g}$,

$$\begin{aligned} Z_{\mathsf{QNF}}^{\omega;\tilde{g}}(\beta) &\approx \sum_{n=0}^{\infty} e^{\hbar\omega(n+\frac{1}{2})} \cdot \Big(1 - \frac{3\tilde{g}\hbar^2}{4m^2w^2}(1 + 2n + 2n^2) + \mathcal{O}(\tilde{g}^2)\Big) \\ &= \underbrace{Z_{\mathsf{QNF}}^{\omega;\tilde{g}=0}(\beta)}_{[2\sinh(\frac{\beta\hbar\omega}{2})]^{-1}} - \frac{3}{4}\Big(\frac{\tilde{g}\hbar^2}{m^2\omega^2}\Big)e^{\frac{-\beta\hbar\omega}{2}} \sum_{n=0}^{\infty}(1 + 2n + 2n^2)e^{-\beta\hbar\omega n} + \mathcal{O}(\tilde{g})^2. \end{aligned} \tag{4.12}$$

Using the relation $ne^{-\beta\hbar\omega n} = (-\frac{1}{\hbar\omega}\frac{\partial}{\partial\beta})e^{-\beta\hbar\omega n}$ to rewrite the above, and evaluating the derivatives, gives

$$\begin{aligned} Z_{\mathsf{QNF}}^{\omega;\tilde{g}}(\beta) &\approx Z_{\mathsf{QNF}}^{\omega;\tilde{g}=0}(\beta) - \frac{3}{4}\Big(\frac{\tilde{g}\hbar^2}{m^2\omega^2}\Big)e^{\frac{-\beta\hbar\omega}{2}} \times \\ &\qquad \times \Big[1 + 2\Big(-\frac{1}{\hbar\omega}\frac{\partial}{\partial\beta}\Big) + 2\Big(-\frac{1}{\hbar\omega}\frac{\partial}{\partial\beta}\Big)^2\Big] \underbrace{\sum_{n=0}^{\infty} e^{-\beta\hbar\omega n}}_{=[1-e^{-\beta\hbar\omega}]^{-1}} + \mathcal{O}(\tilde{g})^2 \\ &= Z_{\mathsf{QNF}}^{\omega;\tilde{g}=0}(\beta) - \frac{3}{4}\Big(\frac{\tilde{g}\hbar^2}{m^2\omega^2}\Big)\frac{1}{2\sinh(\frac{\beta\hbar\omega}{2})}\frac{\cosh^2(\frac{\beta\hbar\omega}{2})}{\sinh^2(\frac{\beta\hbar\omega}{2})} + \mathcal{O}(\tilde{g}^2) \\ &= Z_{\mathsf{QNF}}^{\omega;\tilde{g}=0}(\beta)\left[1 - \frac{3}{4}\Big(\frac{\tilde{g}\hbar^2}{m^2\omega^2}\Big)\coth^2\left(\frac{\beta\hbar\omega}{2}\right) + \mathcal{O}(\tilde{g}^2)\right] \end{aligned} \tag{4.13}$$

which is identical to 4.9.

4.2 Rate from QNF-PT

The energy spectrum generated by QNF around the saddle (TS) is of the following form (taking $J = pq$):

$$E(J) = E_{TS} + \omega J + \underbrace{gE^{(1)}(J) + g^2E^{(2)}(J) + \mathcal{O}(g^3)}_{\equiv\Delta E(J)} \tag{4.14}$$

where $E^{(i)}$ indicates the ith correction to the spectrum. We use again the baseline formulation of the transition rate, given earlier in 3.23:

$$\Gamma(\beta) = \frac{1}{Z(\beta)} \int_{-\infty}^{\infty} \frac{dE}{2\pi\hbar} T(E) e^{-\beta E} \tag{4.15}$$

with the transmission coefficient $T(E) = \left[1 + e^{-\frac{2\pi}{\hbar\omega}(E - E_{TS})}\right]^{-1}$. We can define $J(E) = (E - E_{TS})/\omega$, such that

$$T(J) = \left[1 + e^{-2\pi J(E)/\hbar}\right]^{-1}. \tag{4.16}$$

Then

$$\begin{aligned}
\Gamma(\beta) &= \frac{1}{Z(\beta)} \int_{-\infty}^{\infty} \frac{dJ}{2\pi\hbar} \frac{dE}{dJ} T(J) e^{-\beta E(J)} \\
&= \frac{1}{Z(\beta)} \int_{-\infty}^{\infty} \frac{dJ}{2\pi\hbar} \frac{1}{1 + e^{-2\pi J/\hbar}} e^{-\beta E(J)} \frac{d}{dJ}\Big(E_{TS} + \omega J + \Delta E(J)\Big) \\
&= \frac{1}{Z(\beta)} \int_{-\infty}^{\infty} \frac{dJ}{2\pi\hbar} \frac{\omega}{1 + e^{-2\pi J/\hbar}} e^{-\beta(E_{TS} + \omega J + \Delta E)} \Big(1 + \frac{1}{\omega} \frac{d}{dJ} \Delta E(J)\Big) \\
&= \frac{1}{Z(\beta)} \int_{-\infty}^{\infty} \frac{dJ}{2\pi\hbar} \frac{\omega}{1 + e^{-2\pi J/\hbar}} e^{-\beta(E_{TS} + \omega J)} \Big(1 - \frac{1}{\beta\omega} \frac{d}{dJ}\Big) e^{-\beta \Delta E(J)}.
\end{aligned} \tag{4.17}$$

To fourth order in QNF, we had the energy spectrum (see (2.44))

$$E(J) = E_{TS} + \omega J + \frac{3g}{2m^2\omega^2}\Big(J^2 - \frac{\hbar^2}{4}\Big) + \mathcal{O}(g^2). \tag{4.18}$$

Acting with the derivative on the exponent and subsequently expanding in terms of g, we continue to develop the rate as

$$\begin{aligned}
\Gamma(\beta) = \frac{1}{Z(\beta)} \int_{-\infty}^{\infty} \frac{dJ}{2\pi\hbar} \frac{\omega}{1 + e^{-2\pi J/\hbar}} e^{-\beta(E_{TS} + \omega J)} \\
\times \left(1 + g\Big(\frac{3\beta\hbar^2}{8m^2\omega^2} + \frac{3}{m^2\omega^3} J - \frac{3\beta}{2m^2\omega^2} J^2\Big) + \mathcal{O}(g^2)\right).
\end{aligned} \tag{4.19}$$

We write J in terms of derivatives: $Je^{-\beta(E_{TS} + \omega J)} = \frac{-1}{\omega}(E_{TS} + \frac{d}{d\beta}) e^{-\beta(E_{TS} + \omega J)}$, allowing us to remove the series expansion from the integral in the following manner:

$$\begin{aligned}
\Gamma(\beta) = \frac{1}{Z(\beta)} \Bigg[1 + g\Big(\frac{3\beta\hbar^2}{8m^2\omega^2} + \frac{3}{m^2\omega^3}\Big(\frac{-1}{\omega}(E_{TS} + \frac{d}{d\beta})\Big) - \frac{3\beta}{2m^2\omega^2}\Big(\frac{-1}{\omega}(E_{TS} + \frac{d}{d\beta})\Big)^2\Big) \\
+ \mathcal{O}(g^2)\Bigg] \times \int_{-\infty}^{\infty} \frac{dJ}{2\pi\hbar} \frac{\omega e^{-\beta(E_{TS} + \omega J)}}{1 + e^{-2\pi J/\hbar}}.
\end{aligned} \tag{4.20}$$

This integral is evaluated to be

$$\int_{-\infty}^{\infty} \frac{dJ}{2\pi\hbar} \frac{\omega e^{-\beta(E_{TS} + \omega J)}}{1 + e^{-2\pi J/\hbar}} = \frac{\omega}{4\pi} \csc\Big(\frac{\beta\hbar\omega}{2}\Big) e^{-\beta E_{TS}}. \tag{4.21}$$

Taking $Z(\beta) = [2\sinh(\frac{\beta\hbar\omega}{2})]^{-1}$ and $g = 0$ recovers the WKB result (3.25):

$$\Gamma^{g=0}_{\text{quantum}}(\beta) = \frac{\omega}{2\pi} \frac{\sinh(\frac{\beta\hbar\Omega}{2})}{\sin(\frac{\beta\hbar\omega}{2})} e^{-\beta E_{TS}}. \tag{4.22}$$

This is the non-interacting quantum rate in ratio to which the non-interacting classical rate and interacting quantum rate are plotted. The former is found by taking $\hbar \to 0$, and recovers (3.11):

$$\Gamma^{g=0}_{\text{classical}}(\beta) = \frac{\omega}{2\pi} e^{-\beta E_{TS}}. \tag{4.23}$$

The latter is calculated by plugging the quantity (4.21) into (4.20) in the case of a 1D system. For a 3D system, the integral in (4.15) is evaluated numerically.

4.3 Transition Rate

Here we present the computational results of a QNF-TST script for Mathematica, developed by Giovanni van Marion. In it, an algorithm employs the methods detailed in chapter 2.6 to transform a Hamiltonian into its QNF (up to a certain order), thereafter computing relevant quantities, such as the energy spectrum, partition function, and transition rates over varying temperature. The Hamiltonian from which most results where obtained is as follows:

$$H = \underbrace{\frac{p_1^2}{2m} - \frac{1}{2}m\omega_1^2 q_1^2}_{\text{saddle}} + \underbrace{\sum_{n=2}^{3}\left(\frac{p_n^2}{2m} + \frac{1}{2}m\omega_n^2 q_n^2\right)}_{\text{2 upward directions}} + H_{\text{interactions}} \tag{4.24}$$

$$H_{\text{interactions}} = \sum_{n=1}^{3}\left(\frac{g_4}{4!}q_n^4\right) + \underbrace{\frac{\lambda_4}{4!}q_1^2 q_2^2 + \frac{\lambda_4}{4!}q_1^2 q_3^2}_{\text{mode couplings}}. \tag{4.25}$$

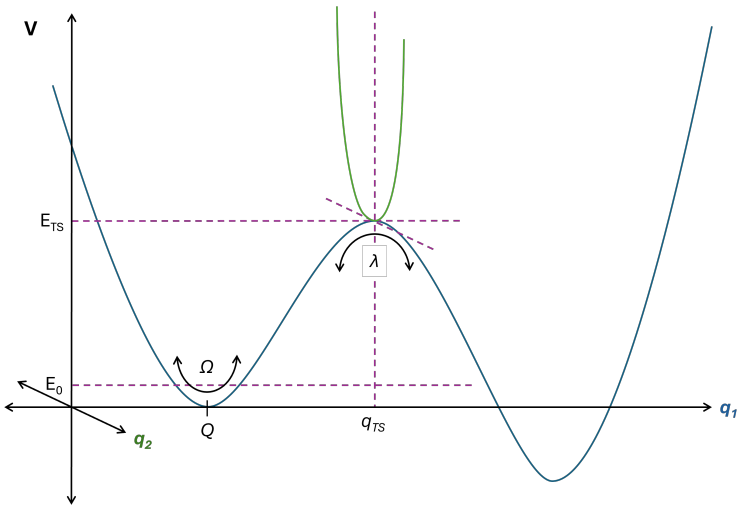

Figure 4.1: Depicting a single additional dimension q_2 with an upward potential ω_2 centered on the saddle point q_{TS}. Here, $\lambda = w_1$ at q_{TS}, and should not be confused with the mode couplings λ_4 in equation 4.25.

It should be noted that the results presented here are of a system with a *harmonic* well and *anharmonic* barrier. There exist separate Mathematica notebooks to compute the partition function of an anharmonic well, which can be combined with the notebook used here to calculate the transition rate for a completely anharmonic system. All

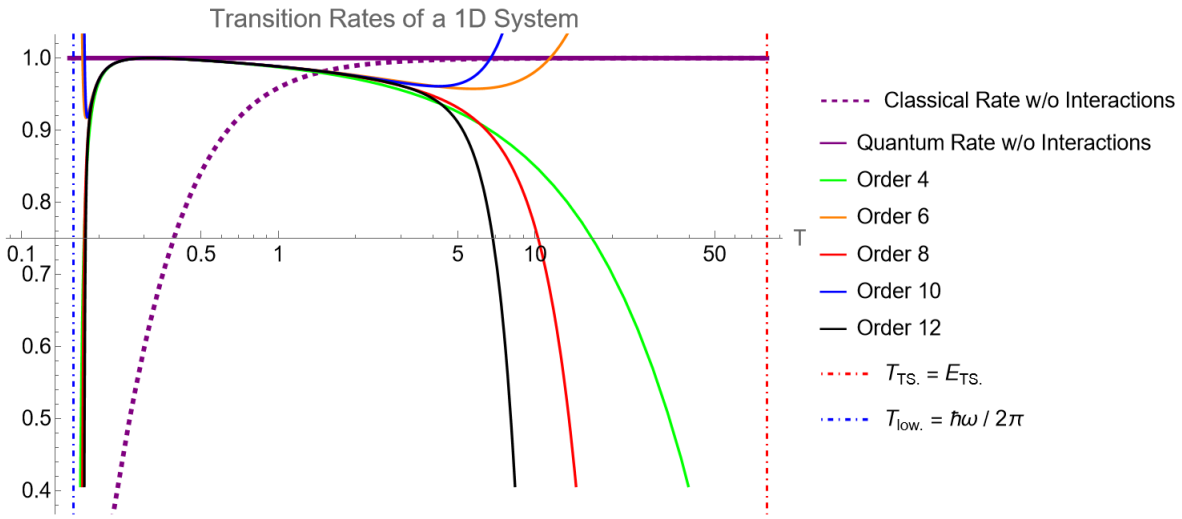

Figure 4.2: Transition rates calculated for a 1D system, with a perturbation parameter $g_4 = 0.005$. Included are the rates of the classical non-interacting system, quantum non-interacting system, and quantum interacting system at QNF-PT orders ranging from 4 to 12. Note that T has units of Joules.

computations were performed with a barrier energy $E_{TS} = 80$, and setting $\hbar = m = 1$. The 1D calculations proved to be a manageable task for the computational power of an average laptop, allowing the investigation of high-order QNF-PT and a wider range of perturbation values. Calculations for the 3D system were restricted to QNF-PT order 8 and lower.

Figure 4.2 gives a general overview of the results, as calculated for a 1D system:

$$H = \frac{p^2}{2m} - \frac{1}{2}m\omega^2 q^2 + g_4 q^4 \tag{4.26}$$

The asymptotic series behaviour is readily apparent, with the highest order QNF-PT terms dictating the direction of growth. One clearly see the temperature regime of validity for the QNF method to indeed lie within the TST boundaries discussed before, $\hbar\omega/2\pi \ll kT \ll E_{TS}$. This may be taken as the interval where all orders coincide to high precision. At very low temperatures, contributions to the transition rate from tunneling are no longer subdominant to classical transitions. At high temperatures (of the same order as the barrier energy), the transition rate is dominated by contributions far above the TS. Thus in these boundary regions, the accuracy of the transition rates presented here is expected to be low.

The dashed purple lines in all these plots, representing the classical rate without interactions, goes to zero at low temperature. This is expected, of course, as there is no tunneling contribution and not enough energy to traverse over the barrier.

Similar behaviour is present in the 3D system, as shown by figure 4.3. The addition of two more dimensions hugely increases the computational load, even requiring different algorithmic methods. As such, rates are calculated for fewer temperature values. One can conclude that, within the estimated domain of QNF-TST validity ($\hbar\omega/2\pi \ll kT \ll E_{TS}$), the QNF-PT order does not have a significant influence on the transition rate accuracy. This is particularly important for consideration of multi-dimensional systems, for which computation times are significantly increased with each increase of normal order.

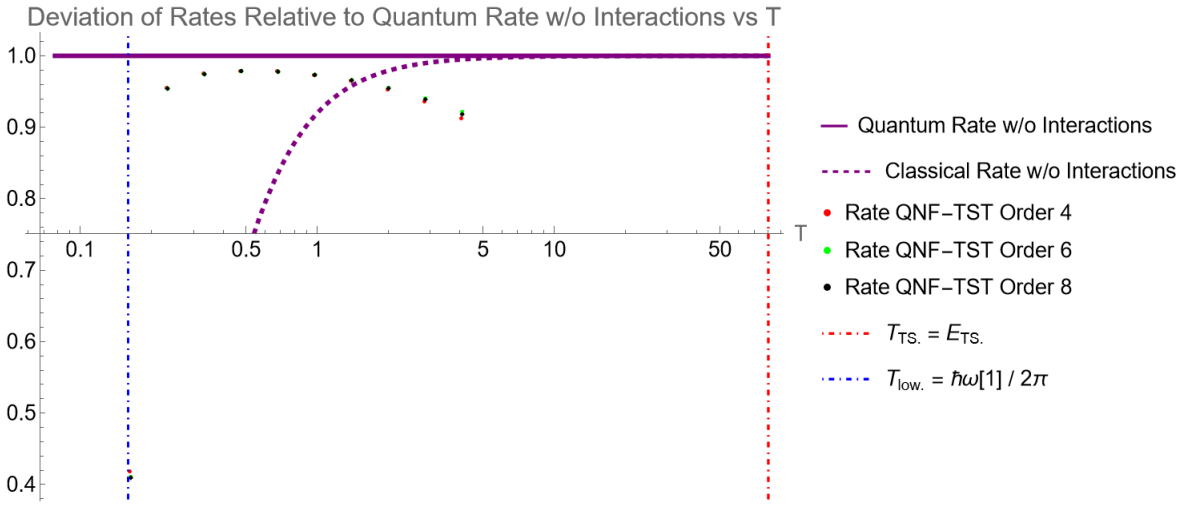

Figure 4.3: The above plot was generated using perturbation and coupling parameters $g_4 = \lambda_4 = 0.1$. The ω_1 refers to the well-saddle 'downward' direction, as opposed to $\omega_{2,3}$ for the two additional 'upward' directions. The rate continues to decrease beyond $T \approx 5$, as shown by figure 4.5.

Consequently, the truncation error of the QNF method is small at these orders, as shown in figure 4.4. Figure 4.5 shows how the truncation error at QNF order 6 (corresponding to the QNF order 8 correction) behaves at temperatures approaching the barrier energy. Initially the error grows as expected, but this does not continue; around $T \simeq 20$, the error begins to shrink. This may be due to competing terms within the correction, however no certain cause is known.

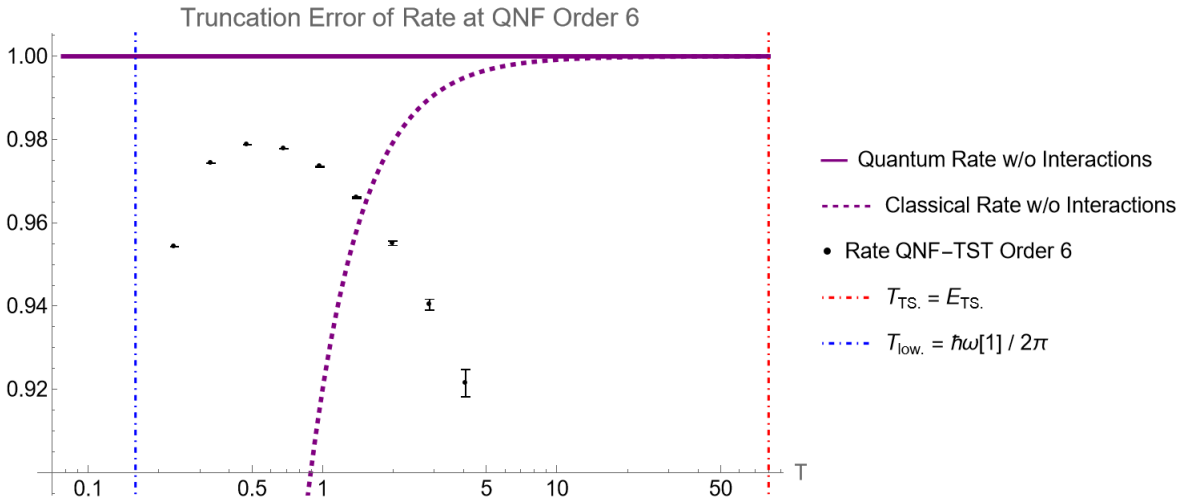

Figure 4.4: Truncation error at QNF order 6, calculated using the same parameter values as for figure 4.3.

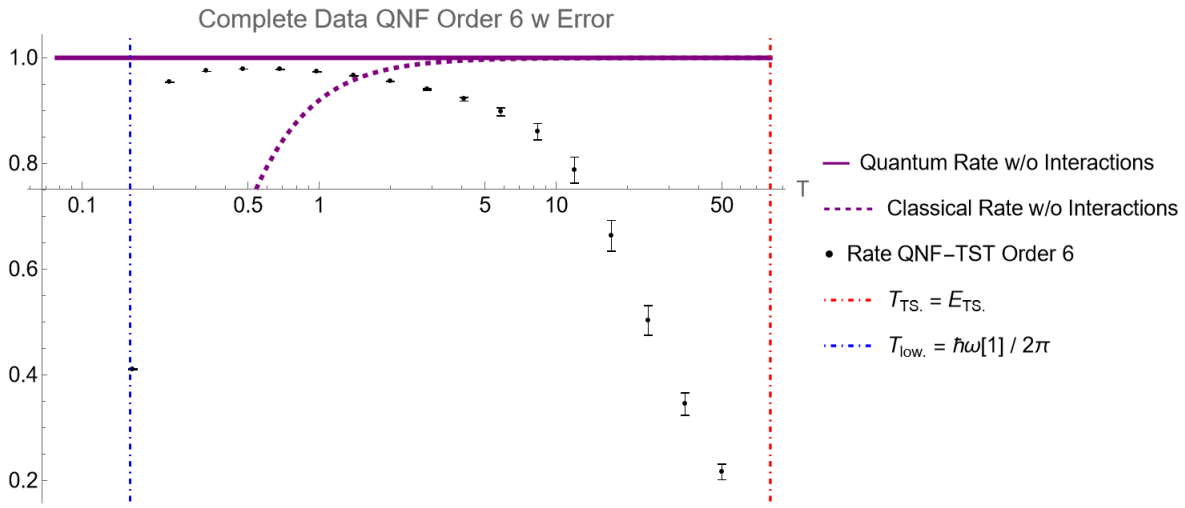

Figure 4.5: Truncation error plot including rates calculated near the barrier energy.

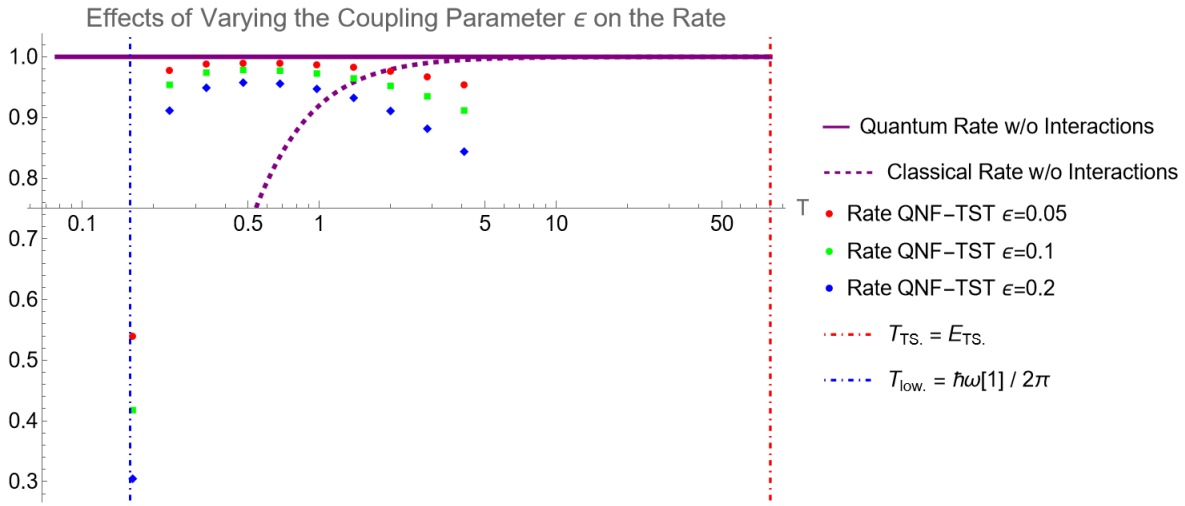

Figure 4.6: Rate calculations with different perturbative parameter values. Here, parameter ϵ represents g_4 and λ_4. These were calculated at QNF order 4, as at a perturbation strength of $\epsilon = 0.2$, results could not be obtained for any higher QNF order due to excessive computation times.

Increasing the size of the perturbation, as shown by figure 4.6, leads to an expectedly larger deviation from the unperturbed (harmonic, non-interacting) case, and also acts to narrow the region of validity for the QNF-PT method.

In 4.25, the coupling between the two upward modes and one downward mode is denoted as λ_4. The effect of inclusion/omission of these interactions on the transition rate is shown in Figure 4.7. There are notable differences between rates at low temperatures, but not at high temperatures. A possible explanation is that states escaping over the saddle have a chance of exciting the coupled upward modes, thus being 'caught', resulting in a decreased transition rate. This may only effect states escaping with low enough energy.

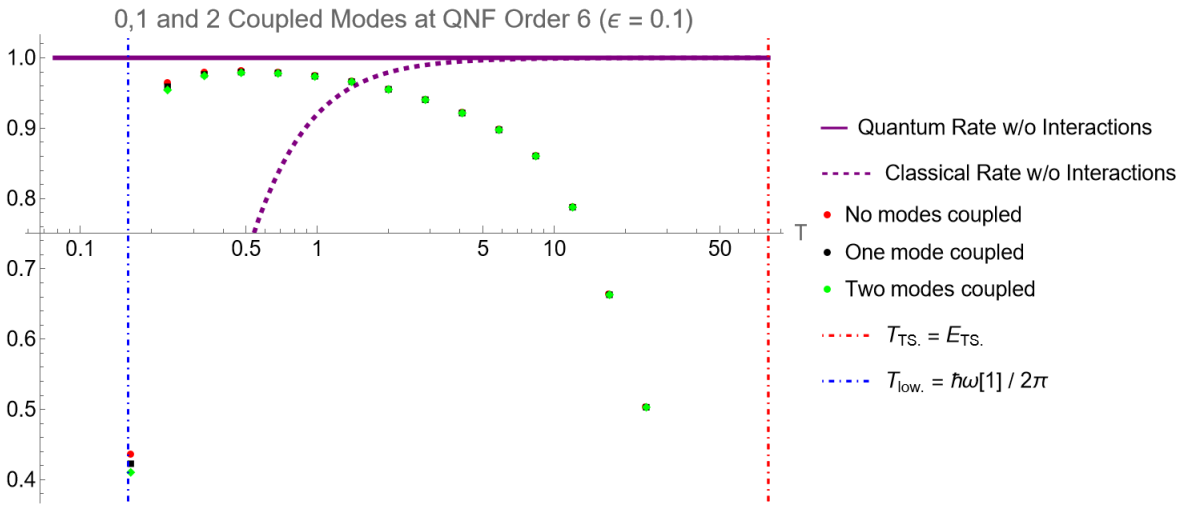

Figure 4.7: Plot demonstrating the effects of coupling 0, 1 or 2 upward modes to a downward mode.

4.4 Mathematica Code:

Herein lies a guide to understanding the Mathematica code developed by Giovanni van Marion, particularly that which is related to finding the QNF Hamiltonian from a given Hamiltonian of regular form. These scripts can find the classical or quantum NF for any finite dimensional Hamiltonian, for local minima or maxima. The notebooks are available on Github: Calculating-Transition-Rates-via-Normal-Forms.

4.4.1 Rescaling and Diagonalizing

```
(*We specify the Hamiltonian in pieces*)
term1 = p[1]^2/(2m) - 1/2 m ω[1]^2×q[1]^2 + p[2]^2/(2m) + 1/2 m ω[2]^2×q[2]^2 + p[3]^2/(2m) + 1/2 m ω[3]^2×q[3]^2;
term2 = 0;
term3 = g4[1]×q[1]^4 /4! + g4[2]×q[2]^4 /4! + g4[3]×q[3]^4 /4! + λ4[1, 2]×q[1]^2×q[2]^2 /4! + λ4[1, 3]×q[1]^2×q[3]^2 /4!;

eigs = {-I ω[1], ω[2], ω[3]};
prs = {{p[1], q[1]}, {p[2], q[2]}, {p[3], q[3]}};

(*Some symplectic transformations used below. x' = (x - I p)/√2 = Sqrt[ħ] a† (the raising operator).
Similarly, p' = (p - I x)/√2 = -I Sqrt[ħ] a (lowering operator).*)
scaleRule = {q[1] → q[1]/Sqrt[m ω[1]],
             p[1] → Sqrt[m ω[1]]p[1],
             q[2] → q[2]/Sqrt[m ω[2]],
             p[2] → Sqrt[m ω[2]]p[2],
             q[3] → q[3]/Sqrt[m ω[3]],
             p[3] → Sqrt[m ω[3]]p[3]};
diagRule = {q[1] → I/Sqrt[2](q[1] + p[1]),
             p[1] → -I/Sqrt[2](p[1] - q[1]),
             q[2] → 1/Sqrt[2](q[2] + I p[2]),
             p[2] → 1/Sqrt[2](p[2] + I q[2]),
             q[3] → 1/Sqrt[2](q[3] + I p[3]),
             p[3] → 1/Sqrt[2](p[3] + I q[3])};
```

Figure 4.8: After defining the Hamiltonian over three terms (1, 2, and 3), it is rescaled and diagonalized by implementing a series of *rules*. These are symplectic transformations analogous to the preparatory steps taken in section 2.3.

```
(*We rescale and diagonalize the Hamiltonian, what we obtain we assign to H[n, m].
Here, n is the order of the term and m is the order of the QNF, which starts at 2.*)
H[0, 2] = 0;
H[1, 2] = 0;
H[2, 2] = Expand[term1 /. scaleRule /. diagRule];
H[3, 2] = Expand[term2 /. scaleRule /. diagRule];
H[4, 2] = Expand[term3 /. scaleRule /. diagRule];
H[n_ ? (# > 4 &), 2] := 0;
```

Figure 4.9: An array, `H[n,m]`, is established as described in the image. This gives the Hamiltonian in QNF order 2, up to qho 4.

The next step is to examine the function `computeQNFSymbUpToOrder`, which will return a given Hamiltonian in its (phase space) QNF up to the desired normal order, specified by the parameter `QNFOrd`. The quantization of the symbols is handled by a subsequent step, described in figure 4.14. Before that, however, we must look into the black box that is `Utils.nb` to trace the calculation of the phase space QNF.

4.4.2 QNF Protocol

The steps to follow are executed within the `Utils.nb` notebook. The function `computeQNFSymbUpToOrder[QNFOrd]` calls upon another function, simply defined as `H`:

```
ClearAll[H]
H[m_, NFOrd_ ? (# ≥ 3 &)] := Expand[mySimplify[Sum[
    1/k! Nest[MB[W[NFOrd], #] &, H[m - k(NFOrd-2), NFOrd-1],
      k],
        {k, 0, Floor[m/(NFOrd-2)]}
]]]
```

Figure 4.10: This function calls several more functions: `mySimplify`, `MB`, and `W`. The latter two reference the *Groenewold-Moyal Bracket* and the symplectic transformation functions W_n, respectively. The former simply collects terms of similar powers and removes those that are zero.

The function `W` merely passes on the results given by another function, `SolveWFromH`, albeit with a minus sign tagged on. Here, the coefficients of the monomials present in H are stored and passed to another function, `getWRulesFromHRules`, which removes null monomials and imposes a scaling defined in `scaleSpecificCoeffs` for the nonzero monomials:

```
ClearAll[scaleSpecificCoeffs]
scaleSpecificCoeffs[pows_ → coeff_] := With[

  {scalar = I eigs.(pows[[1 ;; -1 ;; 2]] - pows[[2 ;; -1 ;; 2]])},
      If[¬ PossibleZeroQ[scalar], pows → coeff / scalar]
 ]

ClearAll[getWRulesFromHRules]
getWRulesFromHRules[coeffRules_] :=
 DeleteCases[scaleSpecificCoeffs /@ coeffRules, Null]

ClearAll[SolveWFromH]
SolveWFromH[H_] := Module[
  {flat = Flatten @ prs, HRules, WRules},
    HRules = CoefficientRules[H, flat];
    WRules = getWRulesFromHRules[HRules];
    FromCoefficientRules[WRules, flat]
]

W[n_] := W[n] = -SolveWFromH[H[n, n - 1]] (*Weird -*)
```

Figure 4.11: Tracing how the symplectic transformation functions W_n are generated within `Utils.nb`.

The Groenewold-Moyal bracket is defined in the `MB` function, in conjunction with the `star` function that represent the star product (see section 2.6 for a reminder):

```
(*STAR PRODUCT*)
ClearAll[star]
star[f_, g_] := Module[
    {pow = 0, partialSum = 0, possibleNextTerm},
    possibleNextTerm = diffOp[f, g, pow];

    While[¬PossibleZeroQ[possibleNextTerm],
        partialSum +=
    1/(pow!) (I ħ/2)^pow possibleNextTerm;
        pow++;
        possibleNextTerm = diffOp[f, g, pow];
    ];

    Return[Expand[partialSum]];
]

(*MOYAL BRACKET*)
ClearAll[MB]
MB[f_, g_] :=
 MB[f, g] = Expand[I/ħ (star[f, g] - star[g, f])]
```

Figure 4.12: While `MB` is rather straightforward, `star` calls upon a specially designed function that deals with the directional derivatives of the Groenewold-Moyal bracket (see figure 4.13).

```
symbRule[n_] := symbRule[n] = With[
    {flat = Flatten @ prs},
    Table[flat[[k]] → Unique[], {k, 1, Length[flat]}]
]

ClearAll[symbRuleInv]
symbRuleInv[n_] := symbRuleInv[n] = Reverse[symbRule[n], 2]

ClearAll[diffOp]
diffOp[f_, g_, 0] :=
 If[PossibleZeroQ[f] ∨ PossibleZeroQ[g], 0, 1]
diffOp[f_, g_, n_] := Module[
    {f1 = f /. symbRule[1],
    g2 = g /. symbRule[2],
    prs1 = prs /. symbRule[1],
    prs2 = prs /. symbRule[2]},
    Return[
        Nest[

       Sum[ D[#, prs1[[k, 2]], prs2[[k, 1]]] -
          D[#, prs1[[k, 1]], prs2[[k, 2]]],
            {k, 1, Length[prs]}] &,
            Times[f1, g2],
            n
        ] /. symbRuleInv[1] /. symbRuleInv[2]
    ];
]
```

Figure 4.13: The function `SymbRule` is used to generate unique tags for the variables with respect to which the right-derivatives act. It's compliment is `symbRuleInv`, which reverses the tag, thereby generating tags for the left-acting derivatives. These are employed in `diffOp`, which calculates the Poisson bracket raised to the nth power.

4.4.3 Quantization

`computeQNFSymbUpToOrder` returns phase space *symbols* p and q. The quantization of these symbols, first collected into $J = pq$ terms, is achieved by the following code:

```
With[{rule = symbRule[45], ruleInv = symbRuleInv[45]},
    ClearAll[JRule];
    JRule = {prs[[1, 1]]×prs[[1, 2]] → J₁, prs[[1, 1]]^n_×prs[[1, 2]]^n_ → J₁^n}
            ~Join~Flatten[Table[{prs[[k, 1]]×prs[[k, 2]] → -I Jₖ,
                                 prs[[k, 1]]^n_×prs[[k, 2]]^n_ → (-I)^n Jₖ^n},
                                 {k, 2, Length[prs]}]] /. rule;
    QNFSymbActions = QNFSymb /. rule //. JRule
]

ClearAll[Op];
Op[J₁, n_] := Expand[OverHat[J₁]×Op[J₁, n-1] - (ℏ/2)^2 (n-1)^2 Op[J₁, n-2]];
Op[J₁, 1] := OverHat[J₁];
Op[J₁, 0] := 1;
Op[Jₘ_/;m≥2, n_] := Expand[OverHat[Jₘ]×Op[Jₘ, n-1] + (ℏ/2)^2 (n-1)^2 Op[Jₘ, n-2]];
Op[Jₘ_/;m≥2, 1] := OverHat[Jₘ];
Op[Jₘ_/;m≥2, 0] := 1;

ClearAll[opRule];
opRule = {Jₘ_ :→ Op[Jₘ, 1], Jₘ_^n_ :→ Op[Jₘ, n]};

QNFActions = QNFSymbActions /. opRule
QNFActions = Expand[QNFActions]

ClearAll[nRule];
nRule = {OverHat[Jₘ_/;m≥2] → ℏ(nₘ + 1/2)};

QNFExplicitQuantumNumbers = Expand[QNFActions /. nRule]
```

Figure 4.14: Symbol actions $J_1 = p_1 q_1$, etc., are established for each dimension of the system, including a factor of $-i$ for the 'upward' directions. Thereafter, the symbols J_1, separately $J_{2,3}$, and powers of these symbols, are made into operators - as in the discussion following equation (2.40). An expression for the explicit quantum numbers is then found by applying the `nRule` substitutions.

5 Conclusion

The author hopes to have introduced the reader to the method of normal forms, its algorithmic procedure, and example applications within a quantum mechanical setting. This was given comparison to the widely studied Feynman diagrammatic method, presenting identical results but with different scenarios of applicability. A review of classical and quantum solutions to the transition rate of a purely harmonic system set the stage for the final investigation into the transition rate of anharmonic systems, wherein the traditional path integral approach is compared to the quantum normal form approach. With this, the Mathematica code developed by Gianni van Marion was employed to calculate the transition rates of one dimensional and three dimensional systems, showcasing the performance of the method over a broad temperature range, various perturbation strengths, and at different normal orders. Some light was shone on the inner workings of this code, so that it may remain an accessible and adaptable tool for future investigations.

The investigation of meta-stable states and their transition rates has widespread applicability. While normal forms may have already reached the mainstream of theoretical techniques in chemistry, particularly in TST, and have been extensively studied in mathematics, physics has yet to confidently adopt the method for the many problems it may address; in nuclear, atomic, and molecular physics. The Mathematica code developed by Gianni van Marion, which works for any finite dimensional system, is a versatile and valuable tool to this end. QNF's adaptation to field theories is an open problem, where it may prove to be a significantly more efficient and more versatile technique to deal with perturbations than the traditional path integral / Feynman diagram methods. Van Marion argued that certain processes in QFTs may be modelled as TST reactions - the false and true vacua being analogous to the reactants and products, with the critical bubble viewed as the TS. Naturally, then, QNF-TST is an attractive framework from which such problems can be tackled. As mentioned in the introduction, one such problem is the phase transition described by the sphaleron - in van Marion's own words;

> *"Possibly a more interesting reaction is sphaleron mediated anomalous Fermion number non-conservation in certain field theories. This is a process in models where crossing a potential energy barrier results in matter turning into antimatter. The TS is this so-called sphaleron, which like the critical bubble is a special localized field configuration. The standard model of particle physics has such a sphaleron in the electroweak sector, which is of interest to those studying the universe's matter-antimatter asymmetry. The canonical rate constant of the process is called the sphaleron rate."*

So indeed, the author hopes to have facilitated the further exploration of this topic, and to have illuminated it for the promising path of research that it is.

A Derivations

A.1 Equation (2.27)

Here the calculation of the terms $\propto C_{3,0}^2$ are shown:

$$\begin{aligned}\mathsf{Mad}_{W_3} H_3^{(2)} &= \{W_3, H_3^{(2)}\}_M \\ &= \sum_{j=0}^{\infty} \frac{(-1)^j (\frac{1}{2}\hbar^{2j})}{(2j+1)!} W_3 \Big[\overleftarrow{\partial_q}\overrightarrow{\partial_p} - \overleftarrow{\partial_p}\overrightarrow{\partial_q}\Big]^{2j+1} H_3^{(2)} \\ &= \Big\{W_3, H_3^{(2)}\Big\} - \frac{\hbar^2}{24} W_3 \Big[\overleftarrow{\partial_q}\overrightarrow{\partial_p} - \overleftarrow{\partial_p}\overrightarrow{\partial_q}\Big]^3 H_3^{(2)}\end{aligned} \tag{A.1}$$

where

$$H_3^{(2)} = C_{3,3}q^3 + C_{3,2}q^2 p + C_{3,1} q p^2 + C_{3,0} p^3 \tag{A.2}$$

and

$$W_3 = -\frac{1}{3}C_{3,3}q^3 - C_{3,2}q^2 p + C_{3,1} q p^2 + \frac{1}{3} C_{3,0} p^3 \tag{A.3}$$

We find

$$\begin{aligned}\Big\{W_3, H_3^{(2)}\Big\} &= \frac{\partial W_3}{\partial q}\frac{\partial H_3^{(2)}}{\partial p} - \frac{\partial W_3}{\partial p}\frac{\partial H_3^{(2)}}{\partial q} \\ &= \lambda^{-1}\Big[2C_{3,2}C_{3,3}q^4 - 8C_{3,1}C_{3,3}q^3 p - 6(C_{3,1}C_{3,2} + C_{3,0}C_{3,3})q^2 p^2 \\ &\qquad - 8C_{3,2}C_{3,0} q p^3 + 2C_{3,1}C_{3,0}p^4\Big] \\ &= \lambda^{-1} C_{3,0}^2 \Big[- 6q^4 - 24 q^3 p + 60 q^2 p^2 - 24 q p^3 - 6p^4\Big]\end{aligned} \tag{A.4}$$

and

$$W_3 \Big[\overleftarrow{\partial_q}\overrightarrow{\partial_p} - \overleftarrow{\partial_p}\overrightarrow{\partial_q}\Big]^3 H_3^{(2)} = 24\lambda^{-1}(C_{3,1}C_{3,2} - C_{3,0}C_{3,3}) = 24\hbar^2 C_{3,0}^2 \cdot (-8) \tag{A.5}$$

such that

$$\mathsf{Mad}_{W_3} H_3^{(2)} = -\lambda^{-1} C_{3,0}^2 \Big[6q^4 + 24 q^3 p - 60 q^2 p^2 + 24 q p^3 + 6p^4 - 8\hbar^2\Big] \tag{A.6}$$

A.2 Equation (2.59)

$$
\begin{aligned}
\langle n|\, x^4\, |m\rangle &= \frac{1}{\sqrt{n!m!}} \langle 0|\, a^n x^4 (a^\dagger)^m\, |0\rangle \\
&= \frac{1}{\sqrt{n!m!}} \left[\binom{1}{0} \langle 0|\, a^{n-1} x^4 a (a^\dagger)^m\, |0\rangle + \binom{1}{1} 4\sqrt{\frac{\hbar}{2m\omega}}\, \langle 0|\, a^{n-1} x^3 (a^\dagger)^m\, |0\rangle \right] \\
&= \frac{1}{\sqrt{n!m!}} \left[\binom{2}{0} \langle 0|\, a^{n-2} x^4 a^2 (a^\dagger)^m\, |0\rangle + \binom{2}{1} 4\sqrt{\frac{\hbar}{2m\omega}}\, \langle 0|\, a^{n-2} x^3 a (a^\dagger)^m\, |0\rangle \right. \\
&\qquad \left. + \binom{2}{2} (4\cdot 3) \left(\sqrt{\frac{\hbar}{2m\omega}}\right)^2 \langle 0|\, a^{n-2} x^2 a (a^\dagger)^m\, |0\rangle \right] \\
&= \frac{1}{\sqrt{n!m!}} \left[\binom{3}{0} \langle 0|\, a^{n-3} x^4 a^3 (a^\dagger)^m\, |0\rangle + \binom{3}{1} 4\sqrt{\frac{\hbar}{2m\omega}}\, \langle 0|\, a^{n-3} x^3 a^2 (a^\dagger)^m\, |0\rangle \right. \\
&\qquad + \binom{3}{2} (4\cdot 3) \left(\sqrt{\frac{\hbar}{2m\omega}}\right)^2 \langle 0|\, a^{n-3} x^2 a (a^\dagger)^m\, |0\rangle \\
&\qquad \left. + \binom{3}{3} (4\cdot 3\cdot 2) \left(\sqrt{\frac{\hbar}{2m\omega}}\right)^3 \langle 0|\, a^{n-3} x a (a^\dagger)^m\, |0\rangle \right] \\
&= \frac{1}{\sqrt{n!m!}} \left[\binom{4}{0} \langle 0|\, a^{n-4} x^4 a^4 (a^\dagger)^m\, |0\rangle + \binom{4}{1} 4\sqrt{\frac{\hbar}{2m\omega}}\, \langle 0|\, a^{n-4} x^3 a^3 (a^\dagger)^m\, |0\rangle \right. \\
&\qquad + \binom{4}{2} (4\cdot 3) \left(\sqrt{\frac{\hbar}{2m\omega}}\right)^2 \langle 0|\, a^{n-4} x^2 a^2 (a^\dagger)^m\, |0\rangle \\
&\qquad + \binom{4}{3} (4\cdot 3\cdot 2) \left(\sqrt{\frac{\hbar}{2m\omega}}\right)^3 \langle 0|\, a^{n-4} x a (a^\dagger)^m\, |0\rangle \\
&\qquad \left. + \binom{4}{4} (4\cdot 3\cdot 2) \left(\sqrt{\frac{\hbar}{2m\omega}}\right)^4 \langle 0|\, a^{n-4} (a^\dagger)^m\, |0\rangle \right]
\end{aligned}
$$

so we see

$$
a^m x^k = \sum_{n=0}^{m} \binom{m}{n} \left(\sqrt{\frac{\hbar}{2m\omega}}\right)^n \left(\frac{d}{dx}\right)^n x^k a^{m-n} \tag{A.7a}
$$

$$
x^k (a^\dagger)^m = \sum_{n=0}^{m} \binom{m}{n} \left(\sqrt{\frac{\hbar}{2m\omega}}\right)^n (a^\dagger)^{m-n} \left(\frac{d}{dx}\right)^n x^k \tag{A.7b}
$$

$$
a^m (a^\dagger)^k = \sum_{n=0}^{m} \binom{m}{n} \left(\frac{d}{da^\dagger}\right)^n (a^\dagger)^k a^{m-n} \tag{A.7c}
$$

so we may rewrite

$$\begin{aligned}
\langle n|\, x^k\, |m\rangle &= \frac{1}{\sqrt{n!m!}} \sum_{i=0}^{n} \binom{n}{i} \left(\sqrt{\frac{\hbar}{2m\omega}}\right)^i \langle 0|\, \left(\frac{d}{dx}\right)^i x^k a^{n-i} (a^\dagger)^m\, |0\rangle \\
&= \frac{1}{\sqrt{n!m!}} \sum_{i=0}^{n} \binom{n}{i} \left(\sqrt{\frac{\hbar}{2m\omega}}\right)^i \sum_{j}^{n-i} \binom{n-i}{j} \langle 0|\, \left(\frac{d}{dx}\right)^i \left(\frac{d}{da^\dagger}\right)^j x^k (a^\dagger)^m a^{n-i-j}\, |0\rangle \\
&= \frac{1}{\sqrt{n!m!}} \sum_{i=0}^{n} \binom{n}{i} \left(\sqrt{\frac{\hbar}{2m\omega}}\right)^i \sum_{j}^{n-i} \binom{n-i}{j} k(k-1)\dots(k-i+1)m(m-1)\dots \\
&\qquad (m-j+1)\, \langle 0|\, x^{k-i} (a^\dagger)^{m-j} a^{n-i-j}\, |0\rangle \\
&= \frac{1}{\sqrt{n!m!}} \sum_{i=0}^{n} \binom{n}{i} \left(\sqrt{\frac{\hbar}{2m\omega}}\right)^i \sum_{j}^{n-i} \binom{n-i}{j} \sum_{l=0}^{m-j} \binom{m-j}{l} \left(\sqrt{\frac{\hbar}{2m\omega}}\right)^l \\
&\qquad \times k(k-1)\dots(k-i+1)m(m-1)\dots(m-j+1)(k-i)(k-i-1)\dots \\
&\qquad\quad \times (k-i-l+1)\, \langle 0|\, (a^\dagger)^{m-j-l} x^{k-i-l} a^{n-i-j}\, |0\rangle
\end{aligned} \tag{A.8}$$

now seeing that the only nonzero terms produced by the sums are those where $j = n-i$, so that $i = n-j$, and $l = m-j$:

$$\begin{aligned}
\langle n|\, x^k\, |m\rangle &= \frac{1}{\sqrt{n!m!}} \sum_{j=0}^{n} \binom{n}{j} \sqrt{\frac{\hbar}{2m\omega}}^{(m+n-2j)} \\
&\qquad \times k\dots(k-m-n+2j+1) \underbrace{m\dots(m-j+1)}_{\frac{m!}{(m-j)!} = j!\binom{m}{j}} \langle 0|\, x^{k-m-n+2j}\, |0\rangle \\
&= \frac{1}{\sqrt{n!m!}} \sum_{j=0}^{\min\{n,m\}} j! \binom{n}{j}\binom{m}{j} \langle 0|\, \left(\sqrt{\frac{\hbar}{2m\omega}}\frac{d}{dx}\right)^{m+n-2j} x^k\, |0\rangle
\end{aligned} \tag{A.9}$$

where the emerging combinatorial factors restrict the sum to the minimum value of $\{n, m\}$.

A.3 Equation (3.42)

Deriving the expression of the classical Euclidean action $S_E[\tilde{x}]$:

From $\mathcal{L}_E = m\dot{x}^2/2 + m\Omega^2 x^2$, one finds the general solution $\tilde{x}(x_f, \tau_f; x_i, \tau_i) = a\cosh\Omega\tau + b\sinh\Omega\tau$. The action is then expressed as:

$$\begin{aligned}
S_E[\tilde{x}(x_f, \tau_f; x_i, \tau_i)] &= \int_{\tau_i}^{\tau_f} d\tau (m\dot{x}^2/2 + m\Omega^2 x^2) \\
&= \frac{m\Omega^2}{2} \int_{\tau_i}^{\tau_f} d\tau \Big((a\sinh\Omega\tau + b\cosh\Omega\tau)^2 + (a\cosh\Omega\tau + b\sinh\Omega\tau)^2 \Big) \\
&= \frac{m\Omega}{2} \Big[2ab \Big(\sinh\Omega(\tau_f + \tau_i) \sinh\Omega(\tau_f - \tau_i) \Big) \\
&\qquad + \Big(a^2 + b^2\Big) \Big(\cosh\Omega(\tau_f + \tau_i) \sinh\Omega(\tau_f - \tau_i) \Big) \Big].
\end{aligned} \tag{A.10}$$

Using $\tau_i = 0$ and $\tau_f = \beta\hbar$, one finds $a = x_i$ and $b = x_f \frac{1}{\sinh \Omega\tau_f} - x_i \frac{\cosh \Omega\tau_f}{\sinh \Omega\tau_f}$. These are then substituted into the expression term by term:

$$2x_i\left(x_f \frac{1}{\sinh \Omega\tau_f} - x_i \frac{\cosh \Omega\tau_f}{\sinh \Omega\tau_f}\right) \sinh^2 \Omega\tau_f = 2x_i x_f \sinh \Omega\tau_f - 2x_i^2 \cosh \Omega\tau_f \sinh \Omega\tau_f \tag{A.11a}$$

$$\begin{aligned}&\left(\left(1 + \frac{\cosh^2 \Omega\tau_f}{\sinh^2 \Omega\tau_f}\right)x_i^2 + \frac{1}{\sinh^2 \Omega\tau_f} x_f^2 - 2\frac{\cosh \Omega\tau_f}{\sinh^2 \Omega\tau_f} x_i x_f\right)(\cosh \Omega\tau_f \sinh \Omega\tau_f) \\ &= \left(\left(1 + \frac{\cosh^2 \Omega\tau_f}{\sinh^2 \Omega\tau_f}\right)x_i^2 + \frac{1}{\sinh^2 \Omega\tau_f} x_f^2\right)(\cosh \Omega\tau_f \sinh \Omega\tau_f) - 2\frac{\cosh^2 \Omega\tau_f}{\sinh \Omega\tau} x_i x_f.\end{aligned} \tag{A.11b}$$

Collect like terms:

$$2x_i x_f \sinh \Omega\tau_f - 2\frac{\cosh^2 \Omega\tau_f}{\sinh \Omega\tau} x_i x_f = -\frac{2x_i x_f}{\sinh \Omega\tau_f} \tag{A.12a}$$

$$\begin{aligned}&\left(\left(1 + \frac{\cosh^2 \Omega\tau_f}{\sinh^2 \Omega\tau_f}\right)x_i^2 + \frac{1}{\sinh^2 \Omega\tau_f} x_f^2\right)(\cosh \Omega\tau_f \sinh \Omega\tau_f) - 2x_i^2 \cosh \Omega\tau_f \sinh \Omega\tau_f \\ &\qquad = (x_i^2 + x_f^2)\frac{\cosh \Omega\tau_f}{\sinh \Omega\tau_f}.\end{aligned} \tag{A.12b}$$

Finally we have

$$S_E[\tilde{x}(x_f, \tau_f; x_i, \tau_i)] = \frac{m\Omega}{2}\left[(x_i^2 + x_f^2)\coth \Omega\tau_f - \frac{2x_i x_f}{\sinh \Omega\tau_f}\right]. \tag{A.13}$$

Bibliography

[1]E. C. Kemble, "The general principles of quantum mechanics. part i", Rev. Mod. Phys. **1**, Publisher: American Physical Society, 157–215 (1929).

[2]H. J. Groenewold, "On the principles of elementary quantum mechanics", Physica **12**, 405–460 (1946).

[3]C. M. Bender and T. T. Wu, "Anharmonic oscillator", Phys. Rev. **184**, 1231–1260 (1969).

[4]A. Bruno, "Analytical form of differential equations", Transactions of the Moscow Mathematical Society **25**, 131–288 (1971).

[5]I. Affleck, "Quantum-statistical metastability", Phys. Rev. Lett. **46**, 388–391 (1981).

[6]R. T. Skodje and D. G. Truhlar, "Parabolic tunneling calculations", J. Phys. Chem. **85**, Publisher: American Chemical Society, 624–628 (1981).

[7]S. Coleman, *Aspects of Symmetry: Selected Erice Lectures* (Cambridge University Press, Cambridge, U.K., 1985).

[8]B. Eckhardt, "Birkhoff-gustavson normal form in classical and quantum mechanics", J. Phys. A: Math. Gen. **19**, 2961–2972 (1986).

[9]K. A. Connors 1932-, *Chemical kinetics : the study of reaction rates in solution*, Section: xiii, 480 pages : illustrations ; 24 cm (VCH, New York, N.Y., 1990).

[10]J. Murdock, "Nonlinear normal forms", in *Normal forms and unfoldings for local dynamical systems* (Springer New York, New York, NY, 2003), pp. 157–293.

[11]R. Pérez-Marco, "Convergence or generic divergence of the birkhoff normal form", Ann. Math. **157**, 557–574 (2003).

[12]A. Zee, *Quantum field theory in a nutshell* (2003).

[13]H. Waalkens, A. Burbanks, and S. Wiggins, "A computational procedure to detect a new type of high-dimensional chaotic saddle and its application to the 3d hill's problem", J. Phys. A: Math. Gen. **37**, L257 (2004).

[14]H. Waalkens, A. Burbanks, and S. Wiggins, "Phase space conduits for reaction in multidimensional systems: HCN isomerization in three dimensions", The Journal of Chemical Physics **121**, 6207–6225 (2004).

[15]H. Waalkens, A. Burbanks, and S. Wiggins, "Escape from planetary neighbourhoods", Monthly Notices of the Royal Astronomical Society **361**, 763–775 (2005).

[16]H. Waalkens, R. Schubert, and S. Wiggins, "Wigner's dynamical transition state theory in phase space: classical and quantum", Nonlinearity **21**, R1–R118 (2008).

[17]R. Rattazzi, "The path integral approach to quantum mechanics lecture notes for quantum mechanics iv", in (2009).

[18]A. Andreassen, D. Farhi, W. Frost, and M. D. Schwartz, "Precision decay rate calculations in quantum field theory", Phys. Rev. D **95**, 085011 (2017).

[19]D. D. Rouwhorst, “Equivalence between the benderwu method and the quantum normal form method”, master (Faculty of Science and Engineering, Groningen, 2017), 36 pp.

[20]R. W. Scholtens, “A transparent view on resonances”, Master’s thesis (University of Groningen, 2022), 104 pp.